MAY 15 1947

# NATIONAL ADVISORY COMMITTEE FOR AERONAUTICS

TECHNICAL NOTE

No. 1282

## SOME CONSIDERATIONS OF THE LATERAL STABILITY OF HIGH-SPEED AIRCRAFT

By Leonard Sternfield

Langley Memorial Aeronautical Laboratory
Langley Field, Va.

Washington
May 1947

N A C A LIBRARY
LANGLEY MEMORIAL AERONAUTICAL
LABORATORY
Langley Field, Va.

NATIONAL ADVISORY COMMITTEE FOR AERONAUTICS

TECHNICAL NOTE NO. 1282

# SOME CONSIDERATIONS OF THE LATERAL STABILITY OF HIGH-SPEED AIRCRAFT

By Leonard Sternfield

## SUMMARY

A theoretical investigation has been made to determine the effect of variations in the lateral-stability derivatives, wing loading, altitude, and radii of gyration on the combination of directional stability and effective dihedral required for lateral stability at the landing and cruising condition. The spiral-stability and oscillatory-stability boundaries were computed for a hypothetical airplane with the wings swept back 60° and of aspect ratio 4 for the case in which the principal longitudinal axis of the airplane is in line with the flight path and also for the case in which the principal axis is inclined above the flight path at the nose, thereby introducing product-of-inertia terms in the lateral equations of motion.

The results of the investigation showed that an airplane with a high wing loading designed for high-speed and high-altitude flight would be laterally stable if the moments of inertia, the location of the principal longitudinal axis of the airplane, and the value of the damping-in-roll derivative $C_{l_p}$ were properly selected. The inclination of the principal longitudinal axis above the flight path at the nose caused a stabilizing shift in the oscillatory-stability boundary but did not affect the spiral-stability boundary. When the principal axis was inclined above the flight path, a stabilizing shift occurred in the oscillatory-stability boundary as either the radius of gyration in roll $k_{X_0}$ or the radius of gyration in yaw $k_{Z_0}$ was reduced; whereas, for the case in which the principal axis was alined with the flight path, the stable region increased as either $k_{Z_0}$ was decreased or $k_{X_0}$ was increased above a critical value. Below this critical value of $k_{X_0}$, a decrease in $k_{X_0}$ increased the stable range of the effective-dihedral derivative $C_{l_\beta}$ for a given directional-stability derivative $C_{n_\beta}$.

As the wing loading or altitude was increased, the stable region decreased. The effect of variations of the stability derivatives was more pronounced for the case of finite product of inertia than for the case of zero product of inertia.

## INTRODUCTION

A theoretical investigation has been carried out to determine the combination of directional stability and effective dihedral required for the lateral stability of aircraft equipped with swept-back wings and designed for high-speed and high-altitude flight. Because very little theoretical or experimental data are available at present on the stability derivatives $C_{l_p}$, $C_{l_r}$, $C_{Y_p}$, and $C_{n_p}$ contributed by swept-back wings, the values of these derivatives were varied in the stability calculations. The investigation also included the effect of altitude, wing loading, radii of gyration, and product of inertia on the lateral-stability boundaries. This paper is an extension of the investigation given in reference 1. Similar investigations are presented in references 2 and 3 but the range of parameters covered herein is of a different order of magnitude from the parameters investigated in references 2 and 3.

Calculations were made of the spiral-stability and oscillatory-stability boundaries for landing and cruising flight for a hypothetical airplane with the wings swept back 60° and of aspect ratio 4, but the conclusions drawn are applicable to any type of airplane characterized by the parameters employed. The results of the computations are plotted as a function of the directional-stability derivative $C_{n_\beta}$ and effective-dihedral derivative $C_{l_\beta}$.

## SYMBOLS AND COEFFICIENTS

$\phi$ angle of bank, radians

$\psi$ angle of azimuth, radians

$\beta$ angle of sideslip, radians $(v/V)$

$v$ sideslip velocity along the Y-axis

$V$ airspeed, feet per second

$\rho$ mass density of air, slugs per cubic foot

| | |
|---|---|
| $q$ | dynamic pressure, pounds per square foot $\left(\frac{1}{2}\rho V^2\right)$ |
| $b$ | wing span, feet |
| $S$ | wing area, square feet |
| $l_t$ | distance from center of gravity of airplane to center of pressure of fin, feet |
| $W$ | weight of airplane, pounds |
| $m$ | mass of airplane, slugs $(W/g)$ |
| $g$ | acceleration of gravity, feet per second per second |
| $\mu$ | relative-density factor $\left(\frac{m}{\rho Sb}\right)$ |
| $\eta$ | angle of attack of principal longitudinal axis of airplane, positive when principal axis is above flight path at the nose, degrees (see fig. 1) |
| $\theta$ | angle between reference axis and horizontal axis, positive when reference axis is above horizontal axis, degrees (see fig. 1) |
| $\epsilon$ | angle between reference axis and principal axis, positive when reference axis is above principal axis, degrees (see fig. 1) |
| $\gamma$ | angle of flight path to horizontal axis, positive in a climb, degrees (see fig. 1) |
| $k_{X_o}$ | radius of gyration in roll about principal longitudinal axis, feet |
| $k_{Z_o}$ | radius of gyration in yaw about principal normal axis, feet |
| $I_{X_o}$ | moment-of-inertia coefficient about principal longitudinal axis $\left(\frac{m{k_{X_o}}^2}{qbS}\right)$ |
| $I_{Z_o}$ | moment-of-inertia coefficient about principal normal axis $\left(\frac{m{k_{Z_o}}^2}{qbS}\right)$ |

$I_X$ moment-of-inertia coefficient about flight-path axis $\left(I_{X_o} \cos^2\eta + I_{Z_o} \sin^2\eta\right)$

$I_Z$ moment-of-inertia coefficient about axis normal to flight path $\left(I_{Z_o} \cos^2\eta + I_{X_o} \sin^2\eta\right)$

$I_{XZ}$ product-of-inertia coefficient with respect to flight-path axis and axis normal to flight path $\left(-\left(I_{Z_o} - I_{X_o}\right) \sin\eta \cos\eta\right)$

$C_L$ trim lift coefficient $\left(\frac{W \cos\gamma}{qS}\right)$

$C_l$ rolling-moment coefficient $\left(\frac{\text{Rolling moment}}{qSb}\right)$

$C_n$ yawing-moment coefficient $\left(\frac{\text{Yawing moment}}{qSb}\right)$

$C_Y$ lateral-force coefficient $\left(\frac{\text{Lateral force}}{qS}\right)$

$r, \dot{\psi}$ yawing angular velocity, radians per second $(d\psi/dt)$

$p, \dot{\phi}$ rolling angular velocity, radians per second $(d\phi/dt)$

$C_{l_\beta}$ effective-dihedral derivative, rate of change of rolling-moment coefficient with angle of sideslip, per radian $\left(\partial C_l/\partial\beta\right)$

$C_{n_\beta}$ directional-stability derivative, rate of change of yawing-moment coefficient with angle of sideslip, per radian $\left(\partial C_n/\partial\beta\right)$

$C_{Y_\beta}$ lateral-force derivative, rate of change of lateral-force coefficient with angle of sideslip, per radian $\left(\partial C_Y/\partial\beta\right)$

$C_{n_r}$ damping-in-yaw derivative, rate of change of yawing-moment coefficient with yawing-angular-velocity factor, per radian $\left(\partial C_n/\partial\frac{rb}{2V}\right)$

$C_{n_p}$ rate of change of yawing-moment coefficient with rolling-angular-velocity factor, per radian $\left(\partial C_n / \partial \frac{pb}{2V}\right)$

$C_{l_p}$ damping-in-roll derivative, rate of change of rolling-moment coefficient with rolling-angular-velocity factor, per radian $\left(\partial C_l / \partial \frac{pb}{2V}\right)$

$C_{l_r}$ rate of change of rolling-moment coefficient with yawing-angular-velocity factor, per radian $\left(\partial C_l / \partial \frac{rb}{2V}\right)$

$C_{Y_p}$ rate of change of lateral-force coefficient with rolling-angular-velocity factor, per radian $\left(\partial C_Y / \partial \frac{pb}{2V}\right)$

$C_{Y_r}$ rate of change of lateral-force coefficient with yawing-angular-velocity factor, per radian $\left(\partial C_Y / \partial \frac{rb}{2V}\right)$

$t$ time, seconds

$D$ differential operator $(d/dt)$

$\Lambda$ angle of sweepback, degrees

$A$ aspect ratio of wing

$R$ Routh's discriminant

$\lambda$ complex root of stability equation $(c \pm id)$

$P$ period of oscillation, seconds

$T_{1/2}$ time for amplitude of oscillation to change by factor of 2 (negative value indicates a decrease to half amplitude, positive value indicates an increase to double amplitude)

EQUATIONS OF MOTION

The linearized equations of motion, referred to stability axes, used to calculate the spiral-stability and oscillatory-stability boundaries for any flight condition, are:

Rolling

$$\left(I_X D^2 - C_{l_{\dot{\phi}}} D\right)\phi - \left(I_{XZ} D^2 + C_{l_{\dot{\psi}}} D\right)\psi - C_{l_\beta}\beta = 0$$

Yawing

$$\left(I_Z D^2 - C_{n_{\dot{\psi}}} D\right)\psi - \left(I_{XZ} D^2 + C_{n_{\dot{\phi}}} D\right)\phi - C_{n_\beta}\beta = 0$$

Sideslipping

$$\frac{2b\mu}{V}\left(D\psi + D\beta\right) - \left(C_L + C_{Y_{\dot{\phi}}} D\right)\phi - \left(C_L \tan\gamma + C_{Y_{\dot{\psi}}} D\right)\psi - C_{Y_\beta}\beta = 0$$

where

$$C_{l_{\dot{\phi}}} = C_{l_p}\left(\frac{b}{2V}\right)$$

$$C_{l_{\dot{\psi}}} = C_{l_r}\left(\frac{b}{2V}\right)$$

$$C_{n_{\dot{\phi}}} = C_{n_p}\left(\frac{b}{2V}\right)$$

$$C_{n_{\dot{\psi}}} = C_{n_r}\left(\frac{b}{2V}\right)$$

$$C_{Y_{\dot{\phi}}} = C_{Y_p}\left(\frac{b}{2V}\right)$$

and

$$C_{Y_{\dot{\psi}}} = C_{Y_r}\left(\frac{b}{2V}\right)$$

When $\phi_o e^{\lambda t}$ is substituted for $\phi$, $\psi_o e^{\lambda t}$ for $\psi$, and $\beta_o e^{\lambda t}$ for $\beta$ in the equations written in determinant form, $\lambda$ must be a root of the equation

$$A\lambda^4 + B\lambda^3 + C\lambda^2 + E\lambda + F = 0$$

where

$$A = -I_{XZ}^2 \frac{2b\mu}{V} + I_X I_Z \frac{2b\mu}{V}$$

$$B = -I_{XZ} C_{l_{\dot{\psi}}} \frac{2b\mu}{V} + I_{XZ}^2 C_{Y_\beta} - I_{XZ} C_{n_{\dot{\phi}}} \frac{2b\mu}{V} - I_X C_{n_{\dot{\psi}}} \frac{2b\mu}{V}$$

$$- I_Z C_{l_{\dot{\phi}}} \frac{2b\mu}{V} - I_X I_Z C_{Y_\beta}$$

$$C = I_{XZ} C_{Y_\beta} C_{l_{\dot{\psi}}} + I_{XZ} \frac{2b\mu}{V} C_{l_\beta} + I_{XZ} C_{Y_\beta} C_{n_{\dot{\phi}}} + I_X C_{Y_\beta} C_{n_{\dot{\psi}}}$$

$$+ I_X \frac{2b\mu}{V} C_{n_\beta} + I_Z C_{l_{\dot{\phi}}} C_{Y_\beta} + \frac{2b\mu}{V} C_{l_{\dot{\phi}}} C_{n_{\dot{\psi}}} - \frac{2b\mu}{V} C_{n_{\dot{\phi}}} C_{l_{\dot{\psi}}}$$

$$- I_{XZ} C_{Y_{\dot{\phi}}} C_{n_\beta} - I_Z C_{Y_{\dot{\phi}}} C_{l_\beta} - I_X C_{Y_{\dot{\psi}}} C_{n_\beta} - I_{XZ} C_{Y_{\dot{\psi}}} C_{l_\beta}$$

$$E = -I_{XZ} C_{n_\beta} C_L - I_Z C_{l_\beta} C_L - C_{l_{\dot{\phi}}} C_{n_{\dot{\psi}}} C_{Y_\beta} - C_{l_{\dot{\phi}}} C_{n_\beta} \frac{2b\mu}{V}$$

$$+ C_{n_{\dot{\phi}}} C_{l_{\dot{\psi}}} C_{Y_\beta} + C_{n_{\dot{\phi}}} C_{l_\beta} \frac{2b\mu}{V} - I_{XZ} C_{l_\beta} C_L \tan\gamma - I_X C_{n_\beta} C_L \tan\gamma$$

$$- C_{Y_{\dot{\phi}}} C_{l_{\dot{\psi}}} C_{n_\beta} + C_{Y_{\dot{\phi}}} C_{n_{\dot{\psi}}} C_{l_\beta} + C_{Y_{\dot{\psi}}} C_{l_{\dot{\phi}}} C_{n_\beta} - C_{Y_{\dot{\psi}}} C_{n_{\dot{\phi}}} C_{l_\beta}$$

$$F = C_L \left(C_{l_\beta} C_{n_{\dot{\psi}}} - C_{l_{\dot{\psi}}} C_{n_\beta}\right) + C_L \tan\gamma \left(C_{n_\beta} C_{l_{\dot{\phi}}} - C_{l_\beta} C_{n_{\dot{\phi}}}\right)$$

The conditions necessary for neutral oscillatory stability are that the coefficients A, B, C, and E must be positive and Routh's discriminant, $R = BCE - AE^2 - B^2F$, must equal zero. The condition necessary for neutral spiral stability is $F = 0$. The completely stable region is therefore bounded by the boundaries $R = 0$ and $F = 0$, which are plotted as a function of the directional-stability derivative $C_{n_\beta}$ and the effective-dihedral derivative $C_{l_\beta}$.

## STABILITY DERIVATIVES AND MASS CHARACTERISTICS

The basic values of the stability derivatives and mass characteristics of the hypothetical airplane with the wings swept back 60° are given in table I. The derivatives $C_{n_\beta}$ and $C_{l_\beta}$ are assumed to be variables in the calculations. The effect of the various parameters investigated on the stability boundaries was determined by varying one parameter while the other parameters maintained the values shown in table I.

The values of the parameters that varied from the basic values of table I and the figures in which the results of the calculations are plotted are presented in table II. The values of $\eta$ of 2° and 5° were arbitrarily selected for the investigation. The value of $\eta = 2°$ represents the cruising condition in which the airplane is trimmed at a small angle of attack; whereas the value of $\eta = 5°$ represents the landing condition with flaps down. If for either case, $\eta$ is larger than the values shown in table II, the calculations would indicate a greater increase in the stable region.

## RESULTS AND DISCUSSION

The results of the investigation are presented in a series of figures which show the oscillatory-stability and spiral-stability boundaries as a function of $C_{n_\beta}$ and $C_{l_\beta}$. Figures 2 and 3 show the region of complete stability bounded by the stability boundaries for landing and cruising flight, respectively. The solid $R = 0$ curve of each figure represents the oscillatory-stability boundary for the airplane with its principal axis in line with the flight path; whereas the dashed curve represents the $R = 0$ boundary for the same airplane with the principal axis inclined above the flight path. The angle of attack of the principal longitudinal axis of the airplane $\eta$ is given in each figure. The spiral-stability boundary ($F = 0$) plotted in each figure applies to both sets of calculations since this boundary is not a function of the product of inertia. The wind-tunnel results for a wing swept back 60° (reference 4) indicated a variation of $C_{l_\beta}$ from 0 to -0.23 as $C_L$ increased from 0 to 0.7. The probable range of variation of $C_{n_\beta}$ is from 0.05 to 0.25. With regard to oscillatory stability, therefore, the probable region of the combination of $C_{n_\beta}$ and $C_{l_\beta}$ is located almost entirely in the unstable region for the case in which the principal axis is alined with the flight path but entirely in the stable region for the case in which the principal axis is inclined above the flight path.

The curves shown in figure 4 indicate the factors mainly responsible for the large stabilizing shift in the $R = 0$ boundary for the case in which the principal axis is inclined above the flight path. These curves, labeled 1 to 5 in figure 4, represent the $R = 0$ boundaries obtained by omitting several terms in the expression for $R = 0$. The oscillatory-stability boundaries of figures 2 and 3 are replotted in figures 4(a) and 4(b), respectively, as curves 1 and 5. All the product-of-inertia factors are omitted from the calculations of curve 1 but are included in the calculations for curve 5. The calculations for curve 2 include all the $I_{XZ}$-factors except the factor $I_{XZ}\frac{2b\mu}{V}C_{l_\beta}C_{l_{\dot{\phi}}}$ in the expression for $R = 0$; whereas the calculations for curve 3 include only the terms containing the factor $I_{XZ}\frac{2b\mu}{V}C_{l_\beta}C_{l_{\dot{\phi}}}$. A comparison of curves 2 and 3 in figure 4 shows that the large stabilizing shift in $R = 0$ is caused mainly by the factor $I_{XZ}\frac{2b\mu}{V}C_{l_\beta}C_{l_{\dot{\phi}}}$. If all terms combined with the factor $I_{XZ}\frac{2b\mu}{V}C_{l_\beta}$ but no other product-of-inertia factor occur in the expression for $R = 0$, an additional stabilizing shift in the boundary from curve 3 to curve 4 occurs. This curve 4 is a good approximation of the $R = 0$ equation which includes the terms with all the product-of-inertia factors. Inasmuch as the product of $\frac{2b\mu}{V}$ and any one of the derivatives $C_{n_{\dot{\phi}}}$, $C_{n_{\dot{\psi}}}$, $C_{l_{\dot{\phi}}}$, $C_{l_{\dot{\psi}}}$, $C_{Y_{\dot{\phi}}}$, or $C_{Y_{\dot{\psi}}}$ is independent of $\mu$ and constant for a given $C_L$ $\left(\text{for example, } \frac{2b\mu}{V}C_{l_{\dot{\phi}}} = C_{l_p}C_L\frac{b}{2g}\right)$, it might appear that the factor $I_{XZ}\frac{2b\mu}{V}C_{l_\beta}C_{l_{\dot{\phi}}}$ is independent of $\mu$. This fact is not true, however, because the factor $C_{l_{\dot{\phi}}}$ usually appears in combination with a second $\frac{2b\mu}{V}$-factor having $I_{XZ}\frac{2b\mu}{V}C_{l_\beta}C_{l_{\dot{\phi}}}$ essentially a direct function of $\mu$.

The damping and period of the lateral oscillation in seconds for the basic conditions are shown in figures 5 and 6. The values of $c$ and $d$, the real and imaginary parts of the complex root of the stability equation, are related to the damping and period of the lateral oscillation by the equations

$$P = \frac{6.28}{d}$$

$$T_{1/2} = \frac{0.69}{c}$$

In general the period of the oscillation decreased as $C_{n_\beta}$ or $C_{l_\beta}$ increased and the damping increased with an increase in $C_{n_\beta}$ but decreased with an increase in $C_{l_\beta}$. The effect of product of inertia was to increase the negative slopes of the lines of constant period and also to rotate the lines of constant damping in a stable direction.

## Effect of Stability Derivatives on Stability Boundaries

Although the assumed velocity of the airplane in the cruising condition was supersonic, the component normal to the leading edge of the swept-back wing was subsonic. The values of the derivatives $C_{l_p}$, $C_{l_r}$, and $C_{n_p}$ used in this investigation were obtained from incompressible strip theory with the assumption that the velocity effective in obtaining lift was equal to $V \cos \Lambda$, and the root and tip effects were neglected. The effect of these stability derivatives on the oscillatory-stability boundaries was determined by varying each of the derivatives $C_{l_p}$, $C_{l_r}$, and $C_{n_p}$ independently. The spiral-stability boundary is also affected by these derivatives but the results are not presented because, in general, this boundary is unimportant since the pilot can readily control a spirally unstable airplane.

For the landing condition, the values of $C_{l_r}$ and $C_{n_p}$ were varied ±50 percent but only the variation in the value of $C_{l_r}$ caused any change in the $R = 0$ boundary. Figure 7 shows a slight stabilizing shift in $R = 0$ for $\eta = 0^\circ$ and $5^\circ$ as $C_{l_r}$ is increased. Unpublished wind-tunnel results of a swept-back wing showed that $C_{n_p}$ reversed its sign from negative to positive as $C_L$ was increased and also that the swept-back wing contributed positive $C_{Y_p}$. Supplementary calculations were made to determine the effect of positive $C_{n_p}$ and and positive $C_{Y_p}$ on the $R = 0$ boundary, and the results shown in figures 8 and 9 indicate a slight increase in the stable region for $\eta = 0^{\circ}$ and $5^{\circ}$ as $C_{n_p}$ and $C_{Y_p}$ was increased. The effect of $C_{l_p}$ on the $R = 0$ boundary for an airplane of two different wing loadings, $\frac{W}{S} = 80$ and 120, is shown in figure 10. The lift coefficient of both airplanes was kept the same by increasing the landing speed of the heavier airplane. The results indicate that, for $\eta = 0^{\circ}$, an increase in the airplane wing loading decreased the effect of a variation of $C_{l_p}$ on the oscillatory boundary; whereas for $\eta = 5^{\circ}$, the variation in $C_{l_p}$ caused a proportional shift in $R = 0$, which was independent of wing loading.

For cruising flight and at $\eta = 0^{\circ}$ and $2^{\circ}$, the values of $C_{l_r}$ and $C_{n_p}$ were varied ±50 percent but the results indicated a negligible change in the $R = 0$ boundary. The effect of positive $C_{n_p}$ and positive $C_{Y_p}$ on the $R = 0$ boundary is shown in figures 11 and 12. In both cases the stable region increased as either $C_{n_p}$ or $C_{Y_p}$ was increased. The damping-in-roll derivative $C_{l_p}$ was increased from 0 to -0.394 which resulted in a marked stabilizing shift in the $R = 0$ boundary for $\eta = 2^{\circ}$ but a very slight change in $R = 0$ boundary for $\eta = 0^{\circ}$ (fig. 13). The results in figure 10 for $\eta = 5^{\circ}$ and in figure 13 for $\eta = 2^{\circ}$ confirm the results shown in figure 4 that the stabilizing shift in the $R = 0$ boundary is caused by the factor $I_{XZ}\frac{2b\mu}{V}C_{l_\beta}C_{l_{\dot{\beta}}}$. It is interesting to note that when $\eta = 0^{\circ}$ the derivatives $C_{l_p}$, $C_{l_r}$, and $C_{n_p}$ could be reduced to zero without seriously affecting the oscillatory-stability boundary.

The shift in the oscillatory-stability boundary resulting from the variation of the stability derivatives was generally more pronounced for the case in which the principal axis was inclined above the flight path than for the case in which the principal axis was alined with the flight path $(\eta = 0^{\circ})$.

## Effect of Wing Loading and Altitude

The effect of wing loading on the $R = 0$ boundary was investigated for two distinct cases. In one case the lift coefficient was varied directly with wing loading, thus constant velocity was maintained; whereas in the other case the velocity was varied in such a manner as to maintain the same lift coefficient. Figures 14 and 15 show the results obtained for the case in which the velocity was maintained constant for landing and cruising flight, respectively. Both figures indicate a decrease in the stable region as the wing loading is increased. For $\eta = 0^{\circ}$ the results agree with those obtained in references 2 and 3 where for an increase in $C_L$ or $\mu$ the stable region is shown to decrease. For $\eta = 2^{\circ}$ the stabilizing effect of the factor $I_{XZ}\frac{2b\mu}{V}C_{l_{\beta}}C_{l_{\dot{\phi}}}$, which increases with $\mu$, is introduced in the $R = 0$ calculations. The results indicate, however, that the destabilizing effect of $C_L$ and $\mu$ is more pronounced than the stabilizing effect of the factor $I_{XZ}\frac{2b\mu}{V}C_{l_{\beta}}C_{l_{\dot{\phi}}}$.

The results obtained on the assumption of constant lift coefficient are presented in figure 16 for landing condition and in figure 17 for cruising flight. Figures 16 and 17 show a decrease in the stable region as the wing loading is increased but not so large a decrease as that indicated in figures 14 and 15. The smaller decrease in the stable region is due to the fact that the destabilizing effect of $C_L$ does not appear in the calculations. The reason for the destabilizing shift in $R = 0$ must be attributed to the increase in $\mu$ since $\mu$ is the only variable in the calculations.

As the wing loading increases, the stability boundary never exceeds the boundary labeled "$\frac{W}{S} = \infty$" in figure 17. This boundary is obtained for the condition in which the velocity is changed with wing loading in such a manner as to keep the lift coefficient constant. The only factor in the equations which therefore increases with wing loading is $\frac{2b\mu}{V}$. As shown previously, the product of $\frac{2b\mu}{V}$ and any one of the derivatives $C_{n_{\dot{\phi}}}$, $C_{l_{\dot{\phi}}}$, $C_{n_{\dot{\psi}}}$, $C_{l_{\dot{\psi}}}$, $C_{Y_{\dot{\phi}}}$, or $C_{Y_{\dot{\psi}}}$ is constant for a given $C_L$. The expression for the oscillatory stability boundary for the limiting case $\frac{W}{S} = \infty$ simplifies for the case in which $\eta = 0^{\circ}$ to

$$R = -I_X I_Z C_{Y_\beta} C_{n_\beta} - I_X C_{n_\beta}\left(C_{n_{\dot\psi}}\frac{2b\mu}{V}\right) + I_Z^2 C_{l_\beta} C_L - I_Z C_{l_\beta}\left(C_{n_{\dot\phi}}\frac{2b\mu}{V}\right) = 0$$

For the case in which the principal axis is inclined to the flight path

$$\begin{aligned} R = {} & I_X I_Z \left[-I_X C_{n_\beta} C_{Y_\beta} + I_Z C_{l_\beta} C_L - C_{l_\beta}\left(C_{n_{\dot\phi}}\frac{2b\mu}{V}\right) + I_{XZ} C_{n_\beta} C_L\right] \\ & + I_X I_{XZ}\left[-C_{n_\beta}\left(C_{l_{\dot\psi}}\frac{2b\mu}{V}\right) + I_{XZ} C_{n_\beta} C_{Y_\beta} - C_{n_\beta}\left(C_{n_{\dot\phi}}\frac{2b\mu}{V}\right)\right. \\ & \left. - I_Z C_{l_\beta} C_{Y_\beta} - C_{l_\beta}\left(C_{n_{\dot\psi}}\frac{2b\mu}{V}\right)\right] - I_Z I_{XZ}\left[-C_{l_\beta}\left(C_{l_{\dot\phi}}\frac{2b\mu}{V}\right) - I_{XZ} C_{l_\beta} C_L\right] \\ & + I_{XZ}^2\left[-C_{l_\beta}\left(C_{l_{\dot\psi}}\frac{2b\mu}{V}\right) + I_{XZ} C_{l_\beta} C_{Y_\beta} - C_{n_\beta}\left(C_{l_{\dot\phi}}\frac{2b\mu}{V}\right)\right. \\ & \left. - I_{XZ} C_{n_\beta} C_L\right] - I_X^2 C_{n_\beta}\left(C_{n_{\dot\psi}}\frac{2b\mu}{V}\right) = 0 \end{aligned}$$

The spiral-stability boundary for figures 14 and 16 and for figures 15 and 17 are the same as the curves of $F = 0$ plotted in figures 2 and 3, respectively, and therefore are omitted in figures 14 to 17. This boundary applies to the three values of wing loading investigated inasmuch as $F = 0$ is independent of wing loading.

The effect of altitude on the $R = 0$ boundary was determined on the assumption that the velocity varied with altitude to maintain constant lift coefficient. The computations made for the variation of wing loading while keeping the lift coefficient constant are therefore applicable to show the effect of altitude.

Figures 16 and 17 are replotted in figures 18 and 19 to indicate the effect of altitude on the oscillatory-stability boundary. The wing loading of the airplane in both figures is assumed to be 80. As the altitude was increased, the value of $C_{n_\beta}$ required for oscillatory stability also increased. The boundary for infinite altitude shown in figure 19 was calculated to show that the $R = 0$ boundary would never exceed this boundary as altitude is increased.

## Effect of Radii of Gyration

The present trend is to design high-speed airplanes with long slender fuselages and to equip the airplane with swept-back or low-aspect-ratio wings, which will result in an increase in the radius of gyration in yaw $k_{Z_0}$ and a decrease in the radius of gyration in roll $k_{X_0}$. The ratio $k_{Z_0}/k_{X_0}$ for conventional airplanes is approximately 2 but, for the hypothetical airplane selected for this investigation, the ratio was estimated to be approximately 5.

Effect of $k_{X_0}$ and $k_{Z_0}$.- In figures 20 and 21, representing the cruising condition, $k_{Z_0}$ is varied from 4.82 to 19.28 while $k_{X_0}$ is kept constant and $k_{X_0}$ is varied from 1.01 to 4.04 while $k_{Z_0}$ is kept constant. The results of similar computations for the limiting cases of infinite wing loading or infinite altitude, as described in the section entitled "Effect of Wing Loading and Altitude," are shown in figures 22 and 23 and for the landing condition are shown in figures 24 and 25.

For $\eta = 0^{\circ}$, the $R = 0$ boundaries in figures 20 to 25 indicate that the stable region is increased as either $k_{Z_0}$ is decreased or $k_{X_0}$ is increased above some critical value. In reference 3, however, it was found that an increase in $k_{X_0}$ decreases the stable region. The apparent difference between the two results is due to the more extensive range of parameters used in the present paper. The small values of $k_{X_0}$ considered in reference 3 cause the stability of the airplane motion to depend to a large extent on the damping-in-roll derivative $C_{l_p}$. If $k_{X_0}$ is then increased the effective damping in roll of the system decreases, thus decreasing the stability of the airplane. With further increase in values of $k_{X_0}$, however, a critical value is reached beyond which the stable region increases with $k_{X_0}$. This point is more clearly illustrated by figures 26 and 27. The $R = 0$ boundaries for several values of $k_{X_o}$ but for the same value of $k_{Z_o}$ are plotted in figure 26. Cross plots of figure 26 with $k_{X_o}$ as ordinate and $C_{l_\beta}$ as abscissa are shown in figure 27 for $C_{n_\beta} = 0.1$, 0.3, and 0.5. The circled points in the figure represent the critical values of $k_{X_o}$. Below the critical value of $k_{X_o}$, an increase in $k_{X_o}$ reduces the stable range of $C_{l_\beta}$ for a given $C_{n_\beta}$ but as $k_{X_o}$ increases above the critical value, the stable region increases. As $C_{n_\beta}$ increases the critical point occurs at a smaller value of $k_{X_o}$ and the slope of the curve above the critical point decreases, thus, a larger increase in the stable range of $C_{l_\beta}$ is indicated for the same increment in $k_{X_o}$.

The results in figures 20 to 25, which show that the stable region is increased as either $k_{Z_o}$ is decreased or $k_{X_o}$ increased above some critical value, can be checked by considering the cases in which $k_{X_o}$ or $k_{Z_o}$ are set equal to infinity. In either case the motion is analyzed on the assumption that only two degrees of freedom remain if either $k_{X_o}$ or $k_{Z_o}$ is infinite. If $k_{X_o} = \infty$, the oscillation of the airplane in azimuth as determined by the stability equation

$$\lambda^2 - \left(\frac{C_{n_{\dot\psi}}}{I_Z} + \frac{C_{Y_\beta}}{\frac{2b\mu}{V}}\right)\lambda + \frac{C_{n_{\dot\psi}}C_{Y_\beta}}{I_Z\,\frac{2b\mu}{V}} + \frac{C_{n_\beta}}{I_Z} = 0$$

will always damp provided $C_{n_\beta}$ is positive inasmuch as $C_{n_{\dot\psi}}$ and $C_{Y_\beta}$ are functions of $C_{n_\beta}$. An increase in $k_{X_o}$ therefore increases the stable region. If $k_{Z_o} = \infty$, the expression for the oscillatory-stability boundary is

$$R = -I_X C_{Y_\beta}{}^2 C_{l_{\dot\phi}} - \frac{2b\mu}{V} C_{Y_\beta} C_{l_{\dot\phi}}{}^2 + I_X \frac{2b\mu}{V} C_L C_{l_\beta} = 0$$

For both landing and cruising flight the $R = 0$ boundary almost coincides with the axis $C_{l_\beta} = 0$. As $k_{Z_0}$ increases, therefore, the stable region decreases.

For $\eta = 2^\circ$ or $5^\circ$, the results of the computations shown in figures 20 to 25 indicate an entirely different trend. A stabilizing shift in the oscillatory-stability boundary occurs as either $k_{X_0}$ or $k_{Z_0}$ is decreased, but a larger increase in the stable region is obtained for the case in which $k_{X_0}$ is decreased than for the case in which $k_{Z_0}$ is decreased. These results can be explained by analyzing the effect of variations of $k_{Z_0}$ and $k_{X_0}$ on the product of inertia. With a reduction in either radius of gyration, the airplane can more easily roll or yaw and the inertia-reaction moment due to the product of inertia, caused by the rolling or yawing acceleration, is stabilizing. Also, an increase in the value of the product-of-inertia coefficient

$$I_{XZ} = -\left(I_Z - I_X\right) \sin \eta \cos \eta$$

which has a stabilizing effect on the $R = 0$ boundary, is obtained by an increase in $k_{Z_0}$ or a decrease in $k_{X_0}$. A decrease in $k_{X_0}$, therefore, combines both stabilizing effects and causes a large stabilizing shift in the oscillatory-stability boundary. For a decrease in $k_{Z_0}$ the stabilizing effect of the inertia-reaction moment is opposed by the destabilizing effect caused by a reduction in $I_{XZ}$, but the resultant effect is an increase in the stable region, not so large however as the increase in the stable region obtained by a decrease in $k_{X_0}$.

Effect of ratio $k_{Z_0}/k_{X_0}$.- The $R = 0$ boundaries in figures 20 and 21 are replotted in figure 28 for constant values of the ratio $k_{Z_0}/k_{X_0}$. In this figure there is also a plot of the $R = 0$ boundary of the hypothetical airplane for $k_{X_0} = 2.02$, $k_{Z_0} = 9.64$, and $\frac{k_{Z_0}}{k_{X_0}} = 4.77$. Similar plots based on figures 22 to 25 are presented in figures 29 and 30.

For $\eta = 0^\circ$, a study of the figures indicates that where $k_{X_0}$ is greater than the critical value, the stable region increases as the ratio $k_{Z_0}/k_{X_0}$ decreases. As $k_{Z_0}/k_{X_0}$ is reduced, a greater stabilizing shift in the $R = 0$ boundary is obtained for a decrease in $k_{Z_0}$; as $k_{Z_0}/k_{X_0}$ is increased, a smaller destabilizing shift in $R = 0$ occurs for a decrease in $k_{X_0}$. If the value of $k_{X_0}$ is less than the critical value, the stable region increases as the ratio $k_{Z_0}/k_{X_0}$ decreases by a reduction in the value of $k_{Z_0}$ or as the ratio $k_{Z_0}/k_{X_0}$ increases by a reduction in the value of $k_{X_0}$.

For $\eta = 2^{\circ}$ or $5^{\circ}$, the results of the calculations indicate that the shift in the $R = 0$ boundary is independent of the ratio $k_{Z_0}/k_{X_0}$ but is a function of the individual values of $k_{X_0}$ and $k_{Z_0}$. The previous discussion of the effect of variations of $k_{X_0}$ and $k_{Z_0}$ on the oscillatory-stability boundary is therefore applicable.

## CONCLUSIONS

The effect of various parameters on the combination of directional-stability derivative $C_{n_\beta}$ and effective-dihedral derivative $C_{l_\beta}$ required for lateral-stability boundaries was determined by varying one parameter while the others maintained specified basic values. For the specified values of the fixed parameters the following conclusions were drawn regarding the effects of the parameters that were varied:

1. An airplane with a high wing loading designed for high-speed and high-altitude flight would be laterally stable if the moments of inertia, the location of the principal longitudinal axis of the airplane, and the value of the damping-in-roll derivative $C_{l_p}$ were properly selected.

2. The inclination of the principal longitudinal axis above the flight path at the nose caused a stabilizing shift in the oscillatory-stability boundary but did not affect the spiral-stability boundary. The factor in the expression for the oscillatory-stability boundary $R = 0$ mainly responsible for the large stabilizing shift is

$$I_{XZ} \frac{2b\mu}{V} C_{l_\beta} C_{l_{\dot\phi}}$$

where

$I_{XZ}$ product-of-inertia coefficient

$b$ wing span

$\mu$ relative-density factor

$V$ airspeed

$C_{l_\beta}$ effective-dihedral derivative

$$C_{l_{\dot{\phi}}} = C_{l_p}\left(\frac{b}{2V}\right)$$

3. For zero product of inertia and at low speeds, a variation in the stability derivatives introduced a small change in the oscillatory-stability boundary. As the wing loading was increased, the effect of these derivatives on the boundary decreased. At high speeds, the stability derivatives may be reduced to zero without seriously affecting the oscillatory-stability boundary.

4. When the principal longitudinal axis was inclined above the flight path at the nose, there was a marked increase in the stable region as the derivative $C_{l_p}$ increased, for both landing and cruising flight. A small shift in the oscillatory-stability boundary was caused by changes in the derivatives $C_{n_p}$, $C_{l_r}$, and $C_{Y_p}$ at the landing condition whereas for cruising flight the effect was negligible.

5. For landing and cruising flight, the stable region decreased as either the wing loading or altitude was increased. In the cruising condition, however, the oscillatory-stability boundary approached a limiting curve as the wing loading or altitude increased indefinitely. These results apply for both zero and finite product of inertia.

6. For landing and cruising flight and for zero product of inertia, the stable region was increased when either the radius of gyration in yaw $k_{Z_0}$ was decreased or the radius of gyration in roll $k_{X_0}$ was increased above a critical value. Below this critical

value of $k_{X_0}$, a decrease in $k_{X_0}$ increased the stable range of $C_{l_\beta}$ for a given $C_{n_\beta}$. The calculations made for the case in which the principal axis was above the flight path indicated a stabilizing shift in the oscillatory-stability boundary when either the radius of gyration in roll or yaw was reduced.

Langley Memorial Aeronautical Laboratory
National Advisory Committee for Aeronautics
Langley Field, Va., March 12, 1947

## REFERENCES

1. Sternfield, Leonard: Effect of Product of Inertia on Lateral Stability. NACA TN No. 1193, 1947.

2. Bamber, Millard J.: Effect of Some Present-Day Airplane Design Trends on Requirements for Lateral Stability. NACA TN No. 814, 1941.

3. Bryant, L. W., and Pugsley, A. G.: The Lateral Stability of Highly Loaded Aeroplanes. R. & M. No. 1840, British A.R.C., 1938.

4. Letko, William, and Goodman, Alex: Preliminary Wind-Tunnel Investigation at Low Speed of Stability and Control Characteristics of Swept-Back Wings. NACA TN No. 1046, 1946.

TABLE I.- STABILITY DERIVATIVES AND MASS CHARACTERISTICS

OF HYPOTHETICAL AIRPLANE

| | Landing | Cruising |
|---|---|---|
| W/S, lb/sq ft | 80 | 80 |
| S, sq ft | 100 | 100 |
| b, ft | 20 | 20 |
| A | 4 | 4 |
| $l_t$, ft | 15 | 15 |
| $\rho$, slug/cu ft | 0.0023 | 0.0002 |
| V, ft/sec | 264 | 1465 |
| $\gamma$, deg | 0 | 0 |
| $C_L$ | 1.0 | 0.372 |
| $\mu$ | 54 | 620 |
| $k_{X_0}$, ft | 2.02 | 2.02 |
| $k_{Z_0}$, ft | 9.64 | 9.64 |
| $C_{l_p}$, per radian | -0.197 | -0.197 |
| $C_{l_r}$, per radian | 0.25 | 0.0929 |
| $C_{n_p}$, per radian | -0.0198 | -0.00732 |
| $C_{n_r}$, per radian | $-1.47C_{n_{\beta(tail)}}$ | $-1.47C_{n_{\beta(tail)}}$ |
| $C_{Y_p}$, per radian | 0 | 0 |
| $C_{Y_r}$, per radian | 0 | 0 |
| $C_{Y_\beta}$, per radian | $-1.33C_{n_{\beta(tail)}}$ | $-1.33C_{n_{\beta(tail)}}$ |
| $C_{n_{\beta(fuselage)}}$ | -0.25 | -0.25 |

NATIONAL ADVISORY
COMMITTEE FOR AERONAUTICS

TABLE II.- VALUES OF PARAMETERS VARIED

[For landing, $\eta = 0^{\circ}$ and $5^{\circ}$; for cruising, $\eta = 0^{\circ}$ and $2^{\circ}$]

| | Landing condition | | Cruising condition | |
|---|---|---|---|---|
| | Value | Figure | Value | Figure |
| $C_{l_r}$ | 0.125, 0.375 | 7 | 0.04654, 0.139 | -- |
| $C_{n_p}$ | 0.0198, -0.0099, -0.0297 | 8 | 0.00732, -0.00366, -0.01098 | 11 |
| $C_{Y_p}$ | 0.132, 1.32 | 9 | 0.293, 2.93 | 12 |
| $C_{l_p}$ | 0, -0.0985 | 10 | 0, -0.394 | 13 |
| W/S | 40, 120 | 14, 16 | 18, 40, 120, $\infty$ | 15, 17 |
| $C_L$ | 0.5, 1.5 | 14 | 0.186, 0.558 | 15 |
| $\rho$ | 0.00152 | 18 | 0, 0.00088 | 19 |
| $k_{Z_o}$ | 4.82, 19.28 | 24 | 4.82, 19.28 | 20, 22 |
| $k_{X_o}$ | 1.01, 1.43, 2.86, 4.04 | 25, 26 | 1.01, 4.04 | 21, 23 |
| $\frac{k_{Z_o}}{k_{X_o}}$ | 2.39, 9.54 | 30 | 2.39, 9.54 | 28, 29 |

NATIONAL ADVISORY
COMMITTEE FOR AERONAUTICS

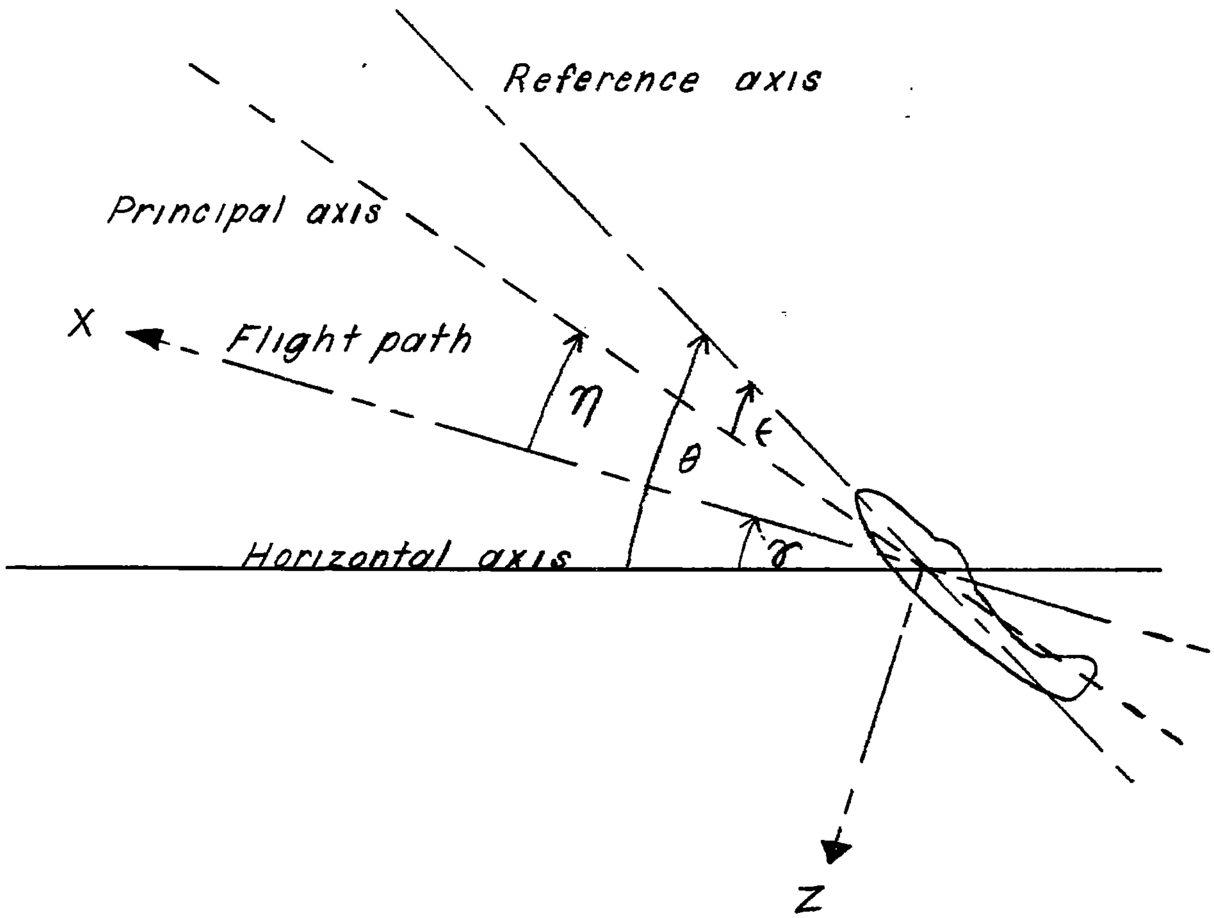


NATIONAL ADVISORY
COMMITTEE FOR AERONAUTICS

Figure 1.— System of axes and angular relationships in flight. Arrows indicate positive direction of angles. $\eta = \theta - \gamma - \epsilon$.

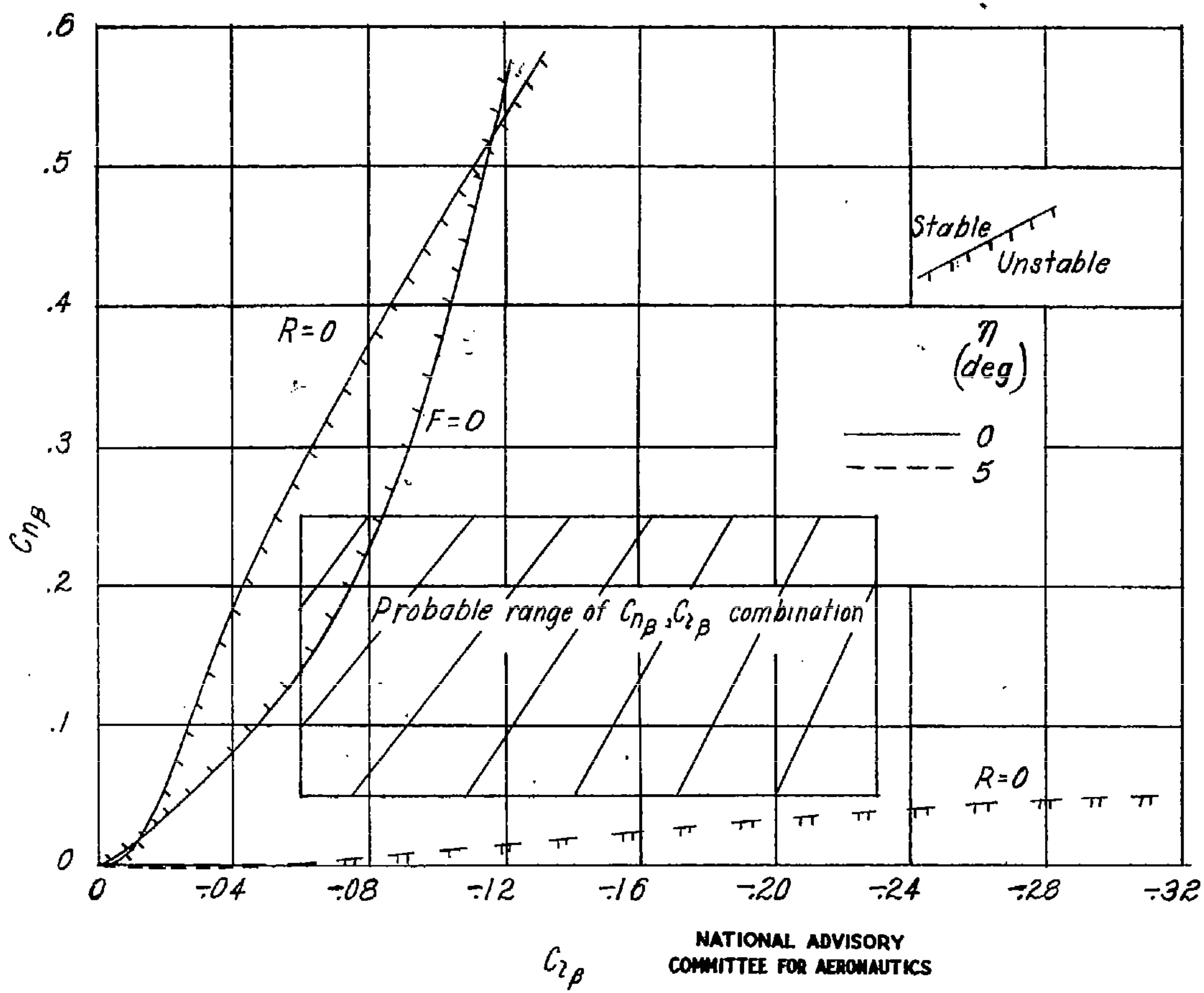


Figure 2.— Lateral-stability boundaries for landing condition. $C_L = 1.0$.

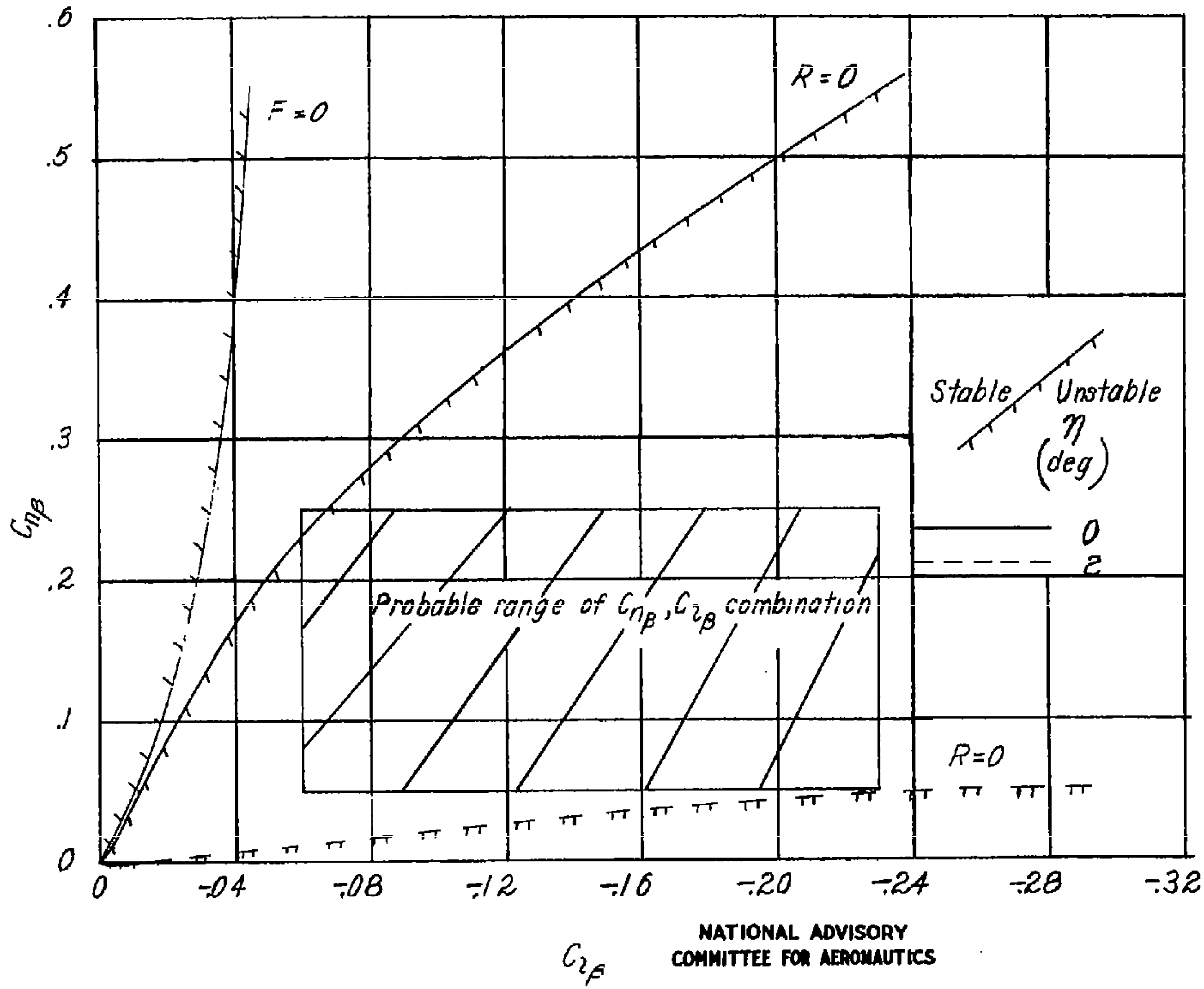


Figure 3.— Lateral-stability boundaries for cruising flight. $C_L = 0.372$.

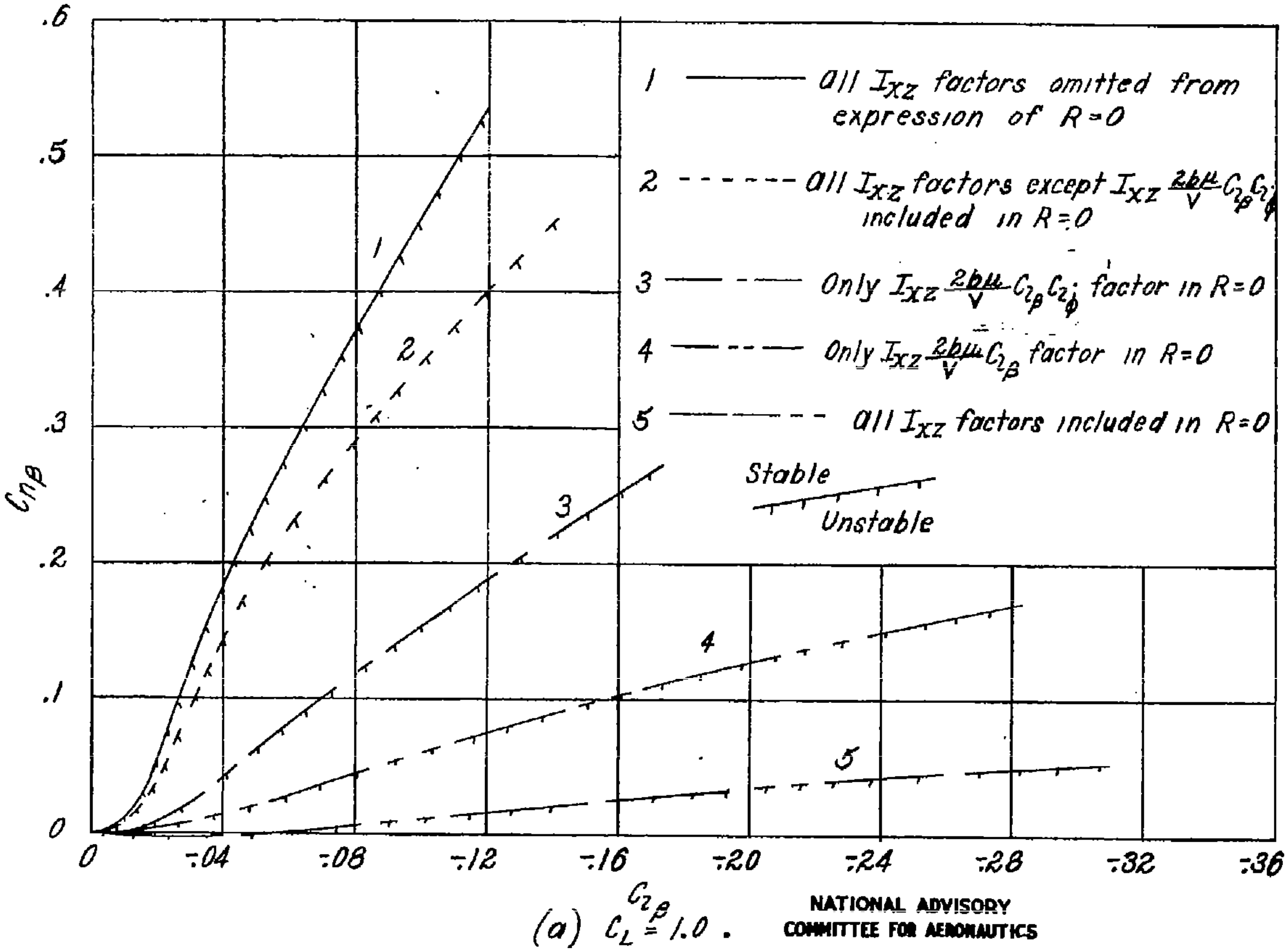


(a) $C_L = 1.0$.

NATIONAL ADVISORY
COMMITTEE FOR AERONAUTICS

Figure 4.— Effect of product-of-inertia factor $I_{XZ}\frac{2b\mu}{V}C_{l_\beta}C_{l_{\dot\phi}}$ on the oscillatory-stability boundary.

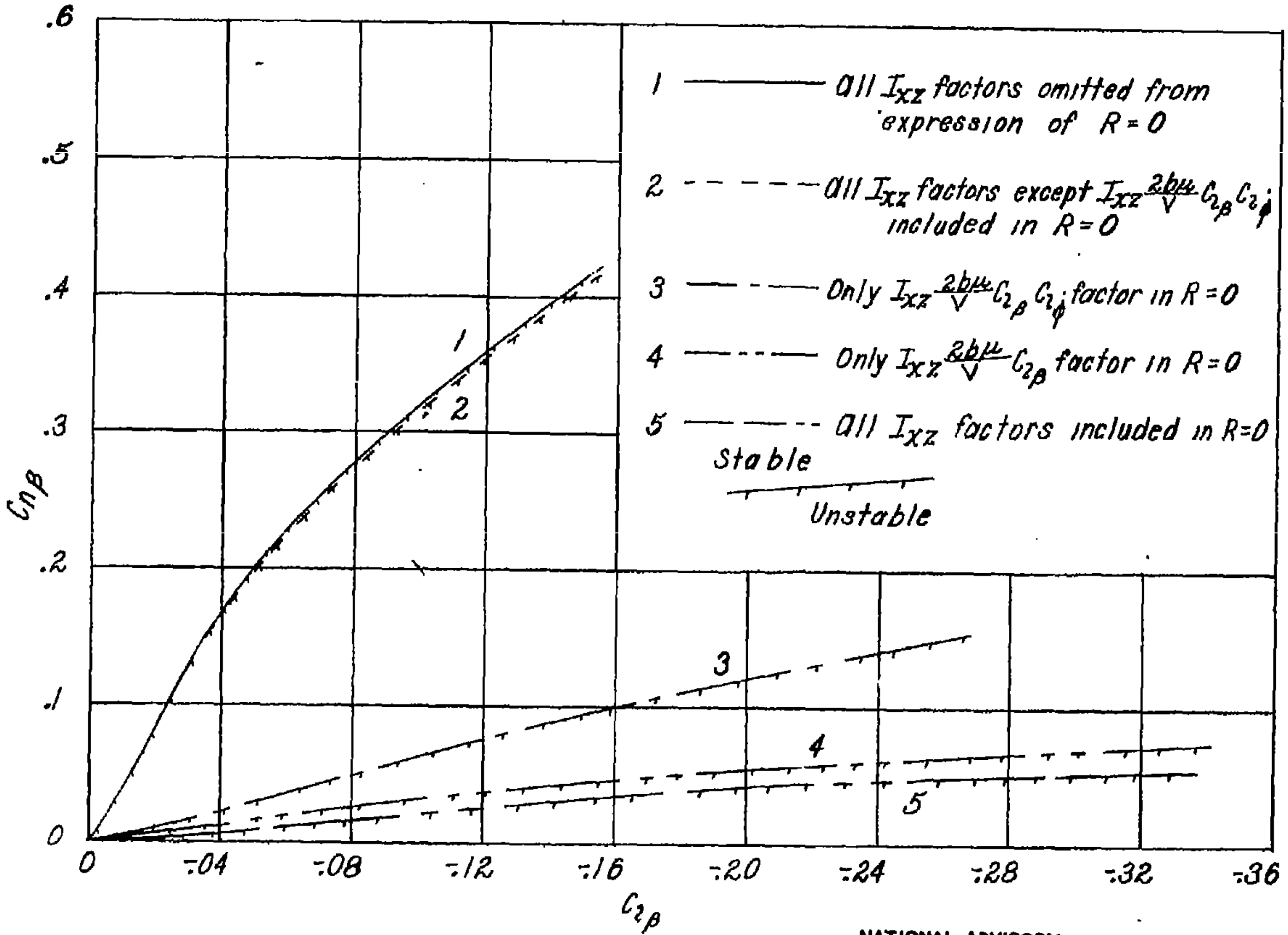


NATIONAL ADVISORY COMMITTEE FOR AERONAUTICS

(b) $C_L = 0.372$.

Figure 4.— Concluded.

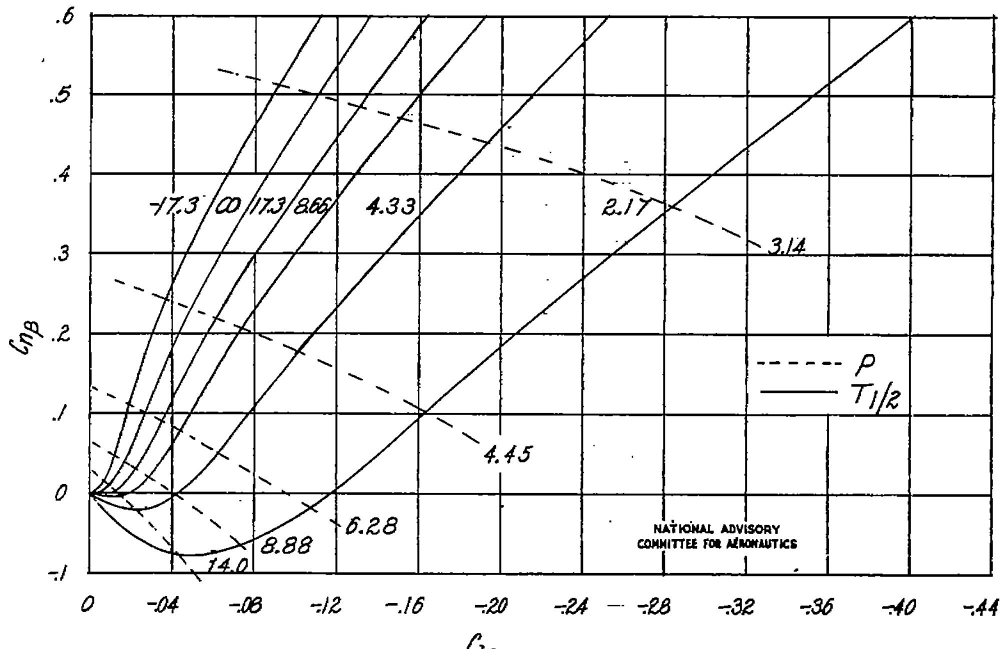


(a) $\eta = 0°$.

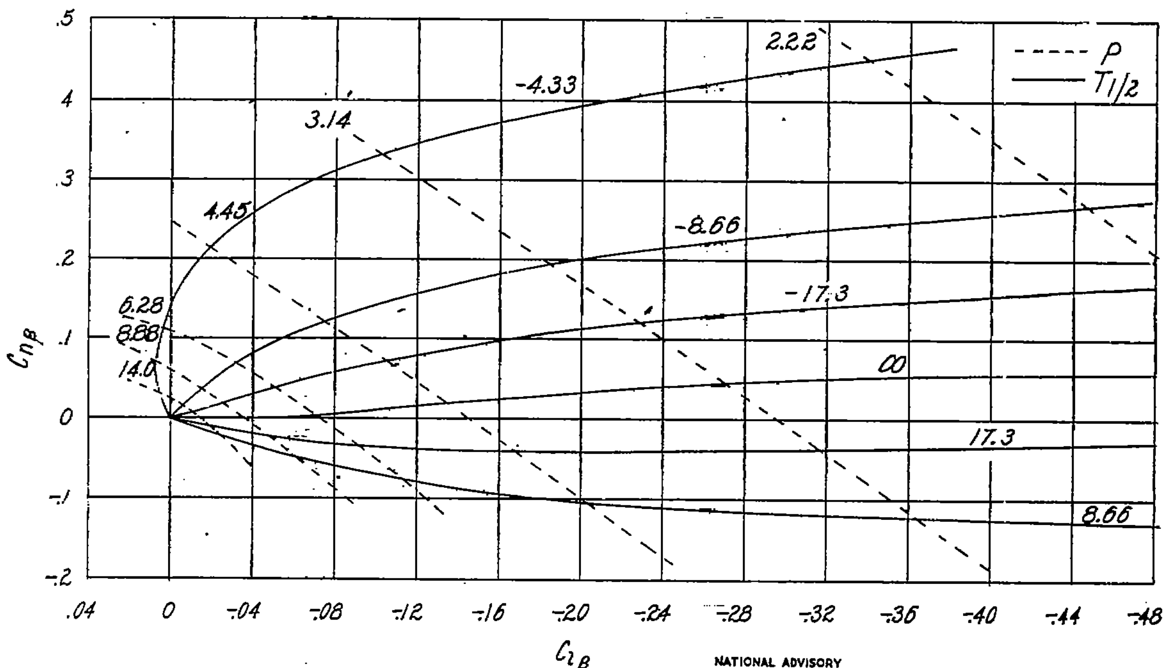


(b) $\eta = 5°$.

Figure 5.— Curves of constant period and constant damping for landing condition. $C_L = 1.0$.

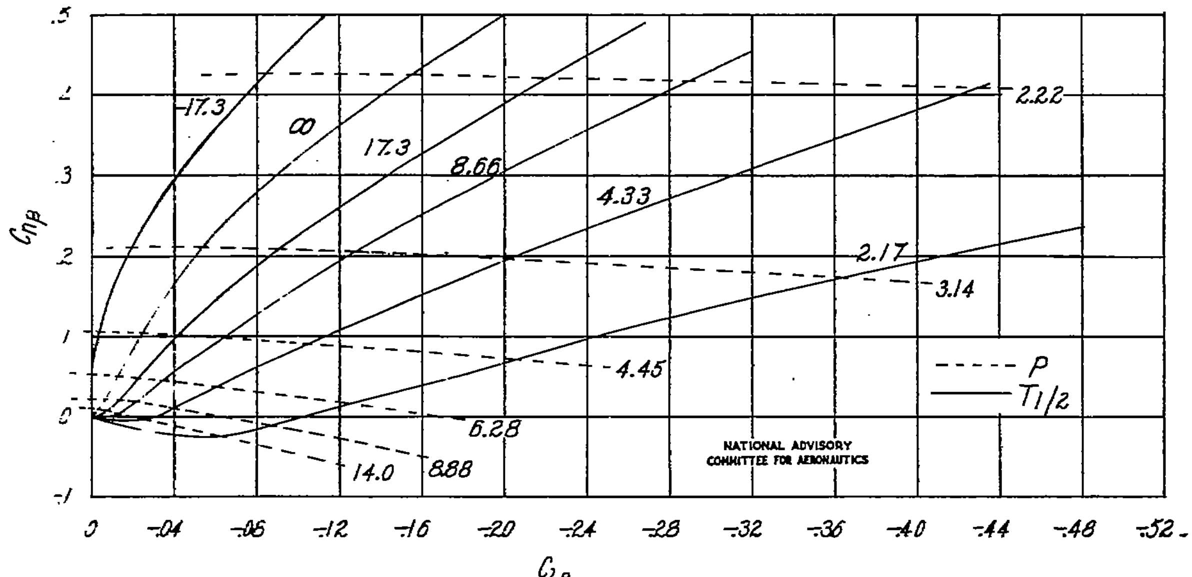


(a) $\eta = 0°$.

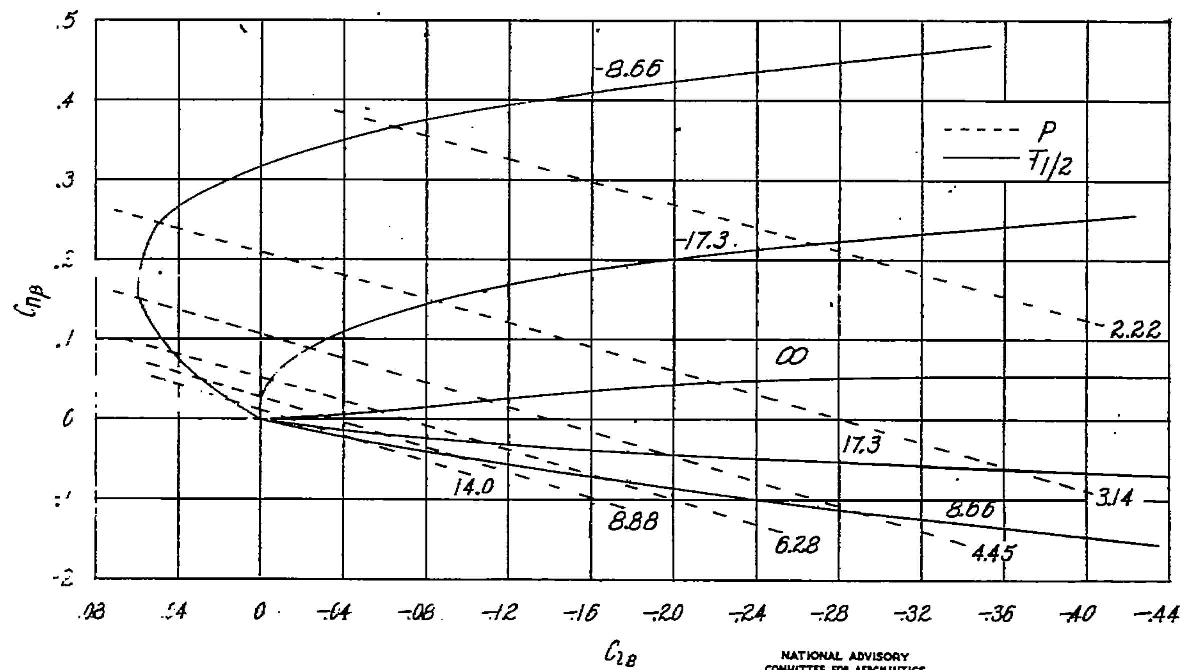


(b) $\eta = 2°$.

Figure 6.— Curves of constant period and constant damping for cruising flight. $C_L = 0.372$.

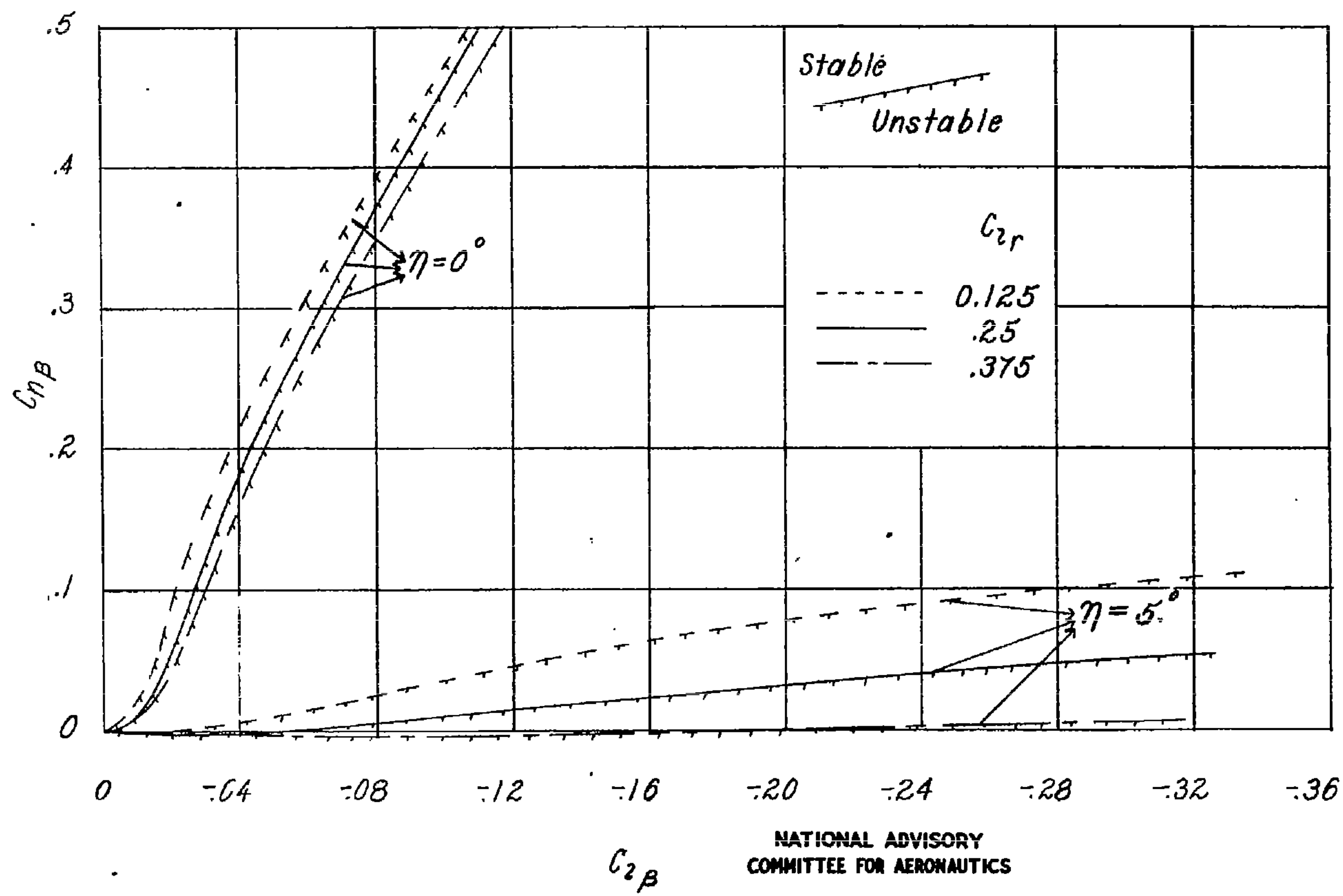


NATIONAL ADVISORY
COMMITTEE FOR AERONAUTICS

Figure 7.— Effect of $C_{l_r}$ on the oscillatory-stability boundary for landing condition. $C_L = 1.0$.

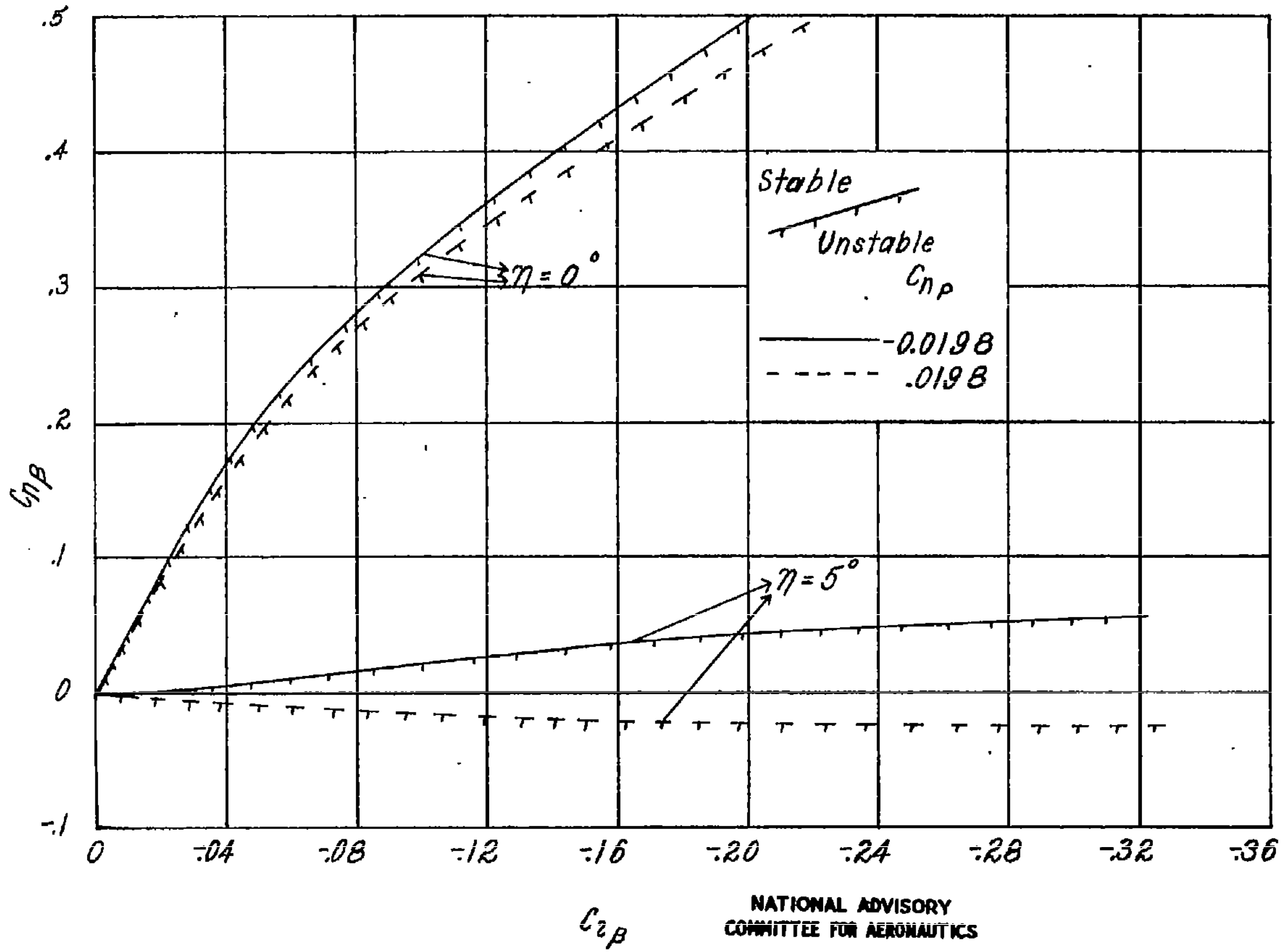


NATIONAL ADVISORY COMMITTEE FOR AERONAUTICS

Figure 8.— Effect of $C_{n_p}$ on the oscillatory-stability boundary for landing condition. $C_L = 1.0$.

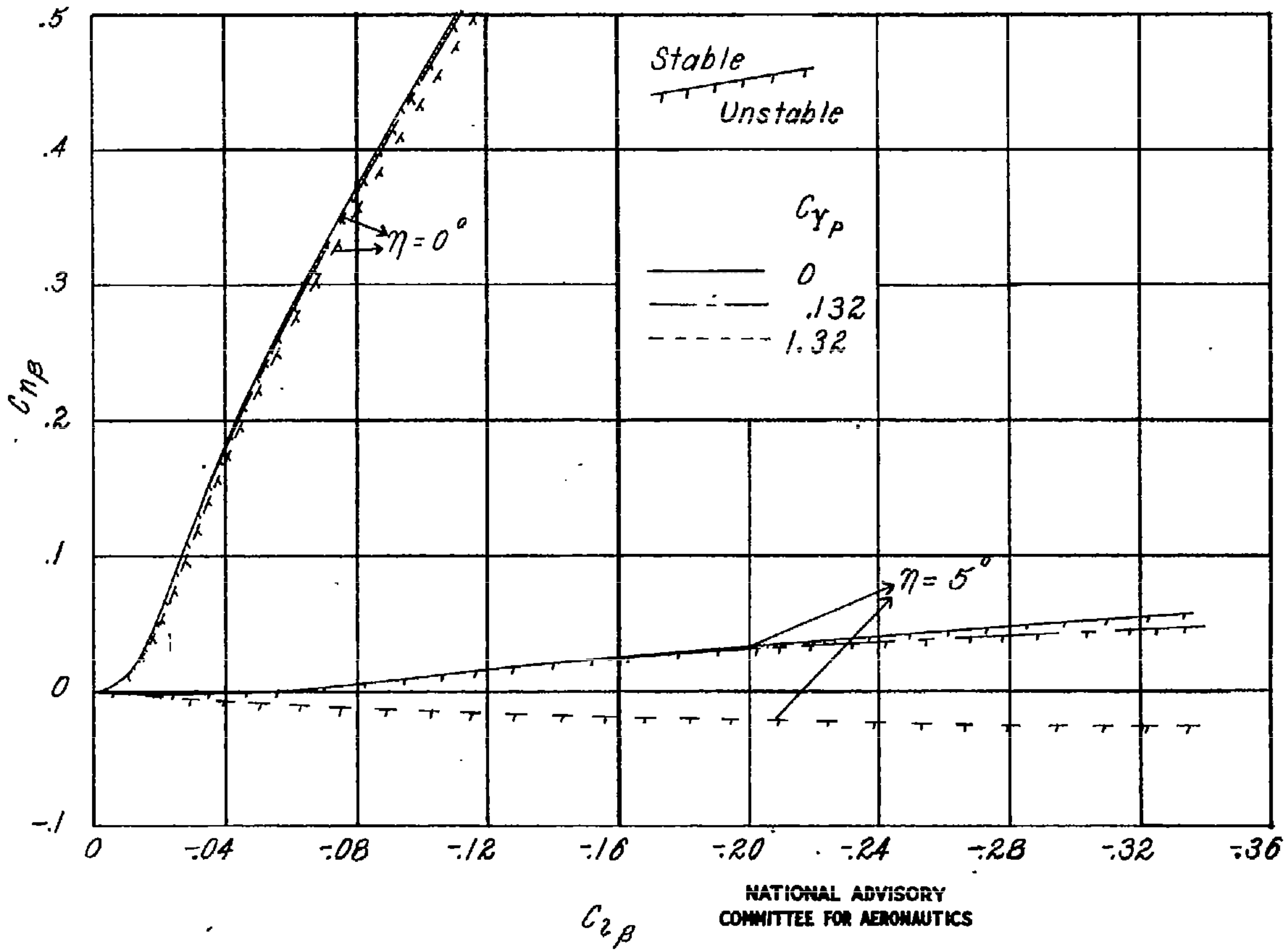


Figure 9.— Effect of $C_{Y_p}$ on the oscillatory-stability boundary for landing condition. $C_L = 1.0$.

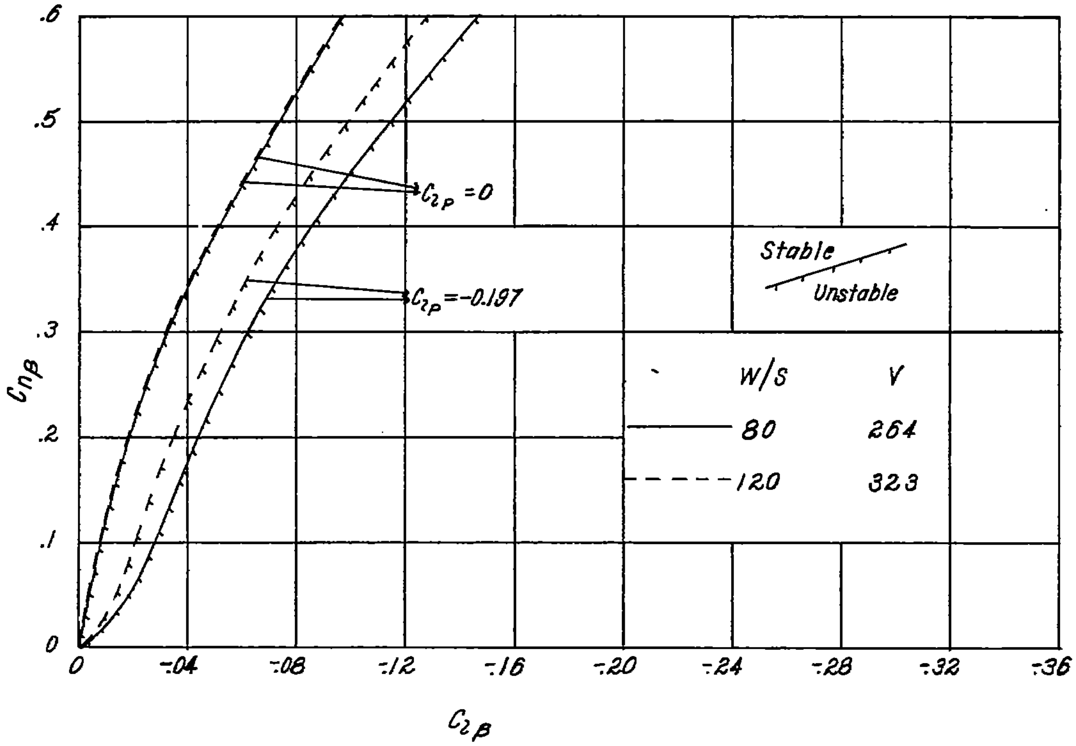


(a) $\eta = 0°$.

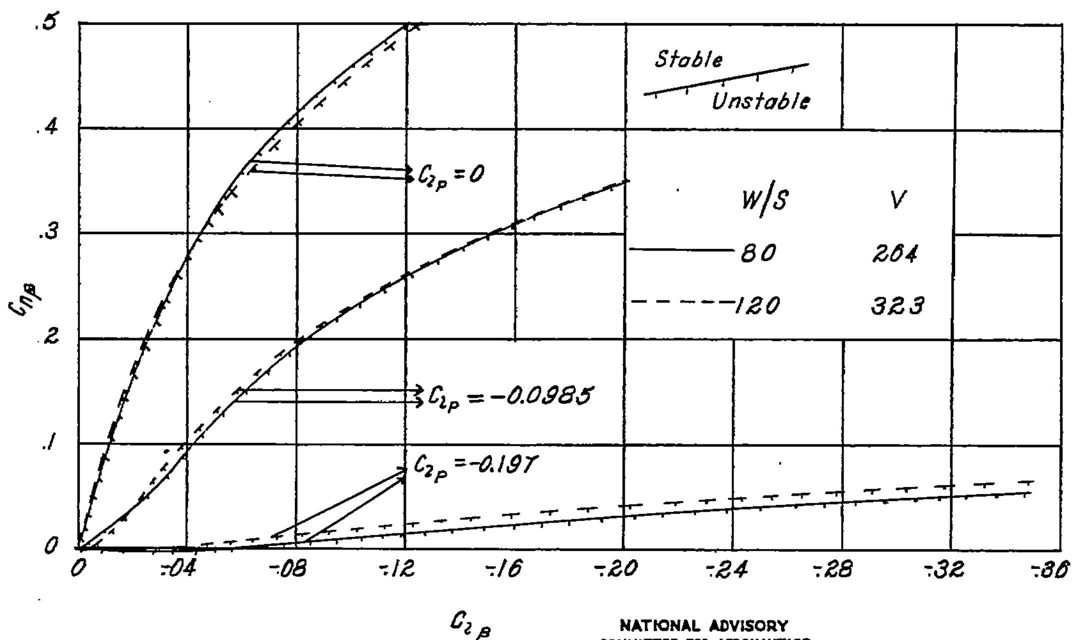


(b) $\eta = 5°$.

NATIONAL ADVISORY COMMITTEE FOR AERONAUTICS

Figure 10.— Effect of damping-in-roll derivative on the oscillatory-stability boundary for landing condition. $C_L = 1.0$.

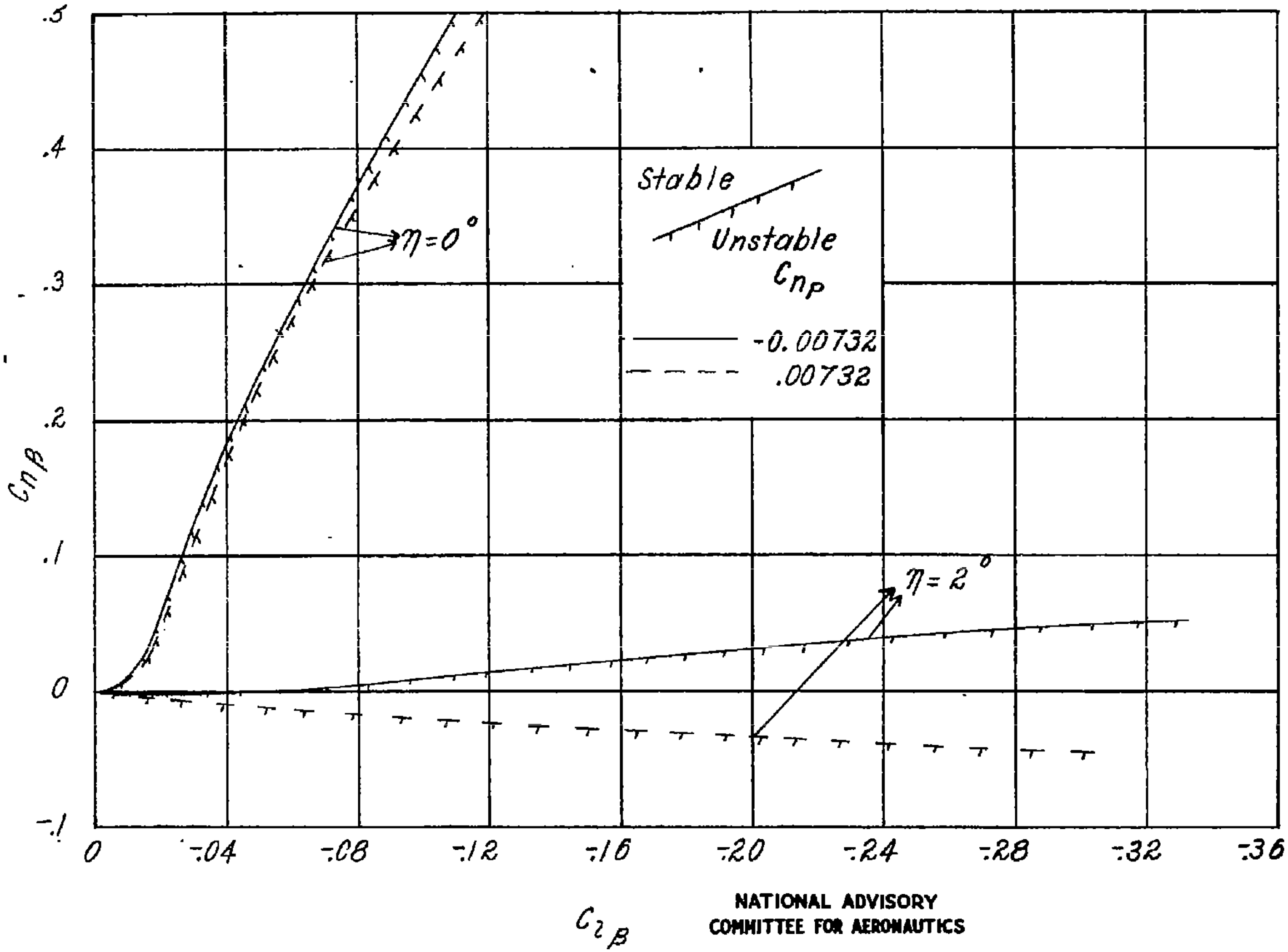


Figure 11.— Effect of $C_{n_p}$ on the oscillatory-stability boundary for cruising flight. $C_L = 0.372$.

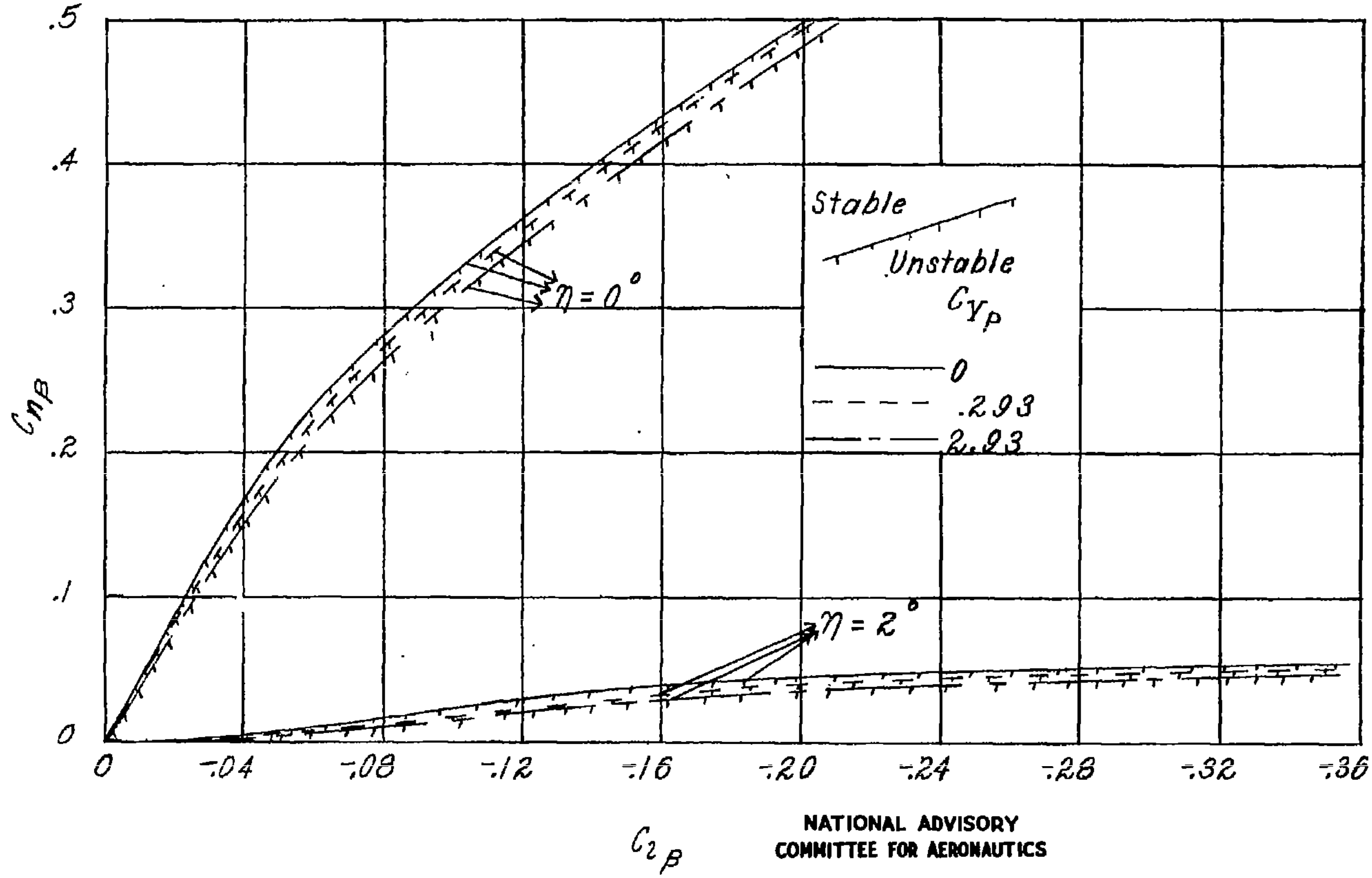


NATIONAL ADVISORY
COMMITTEE FOR AERONAUTICS

Figure 12.— Effect of $C_{Y_p}$ on the oscillatory-stability boundary for cruising flight. $C_L = 0.372$.

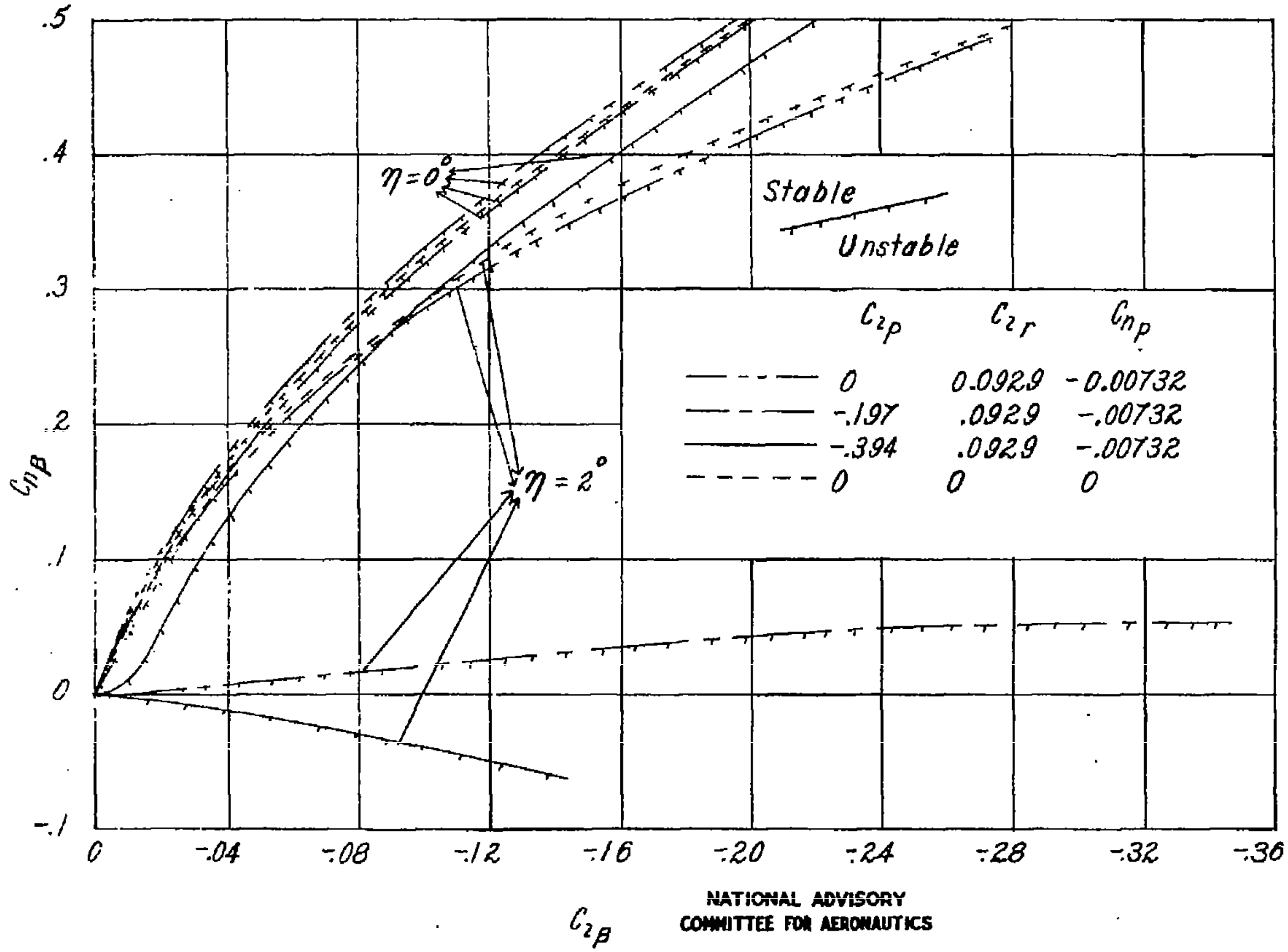


Figure 13.— Effect of stability derivatives on the oscillatory-stability boundary for cruising flight. $C_L = 0.372$.

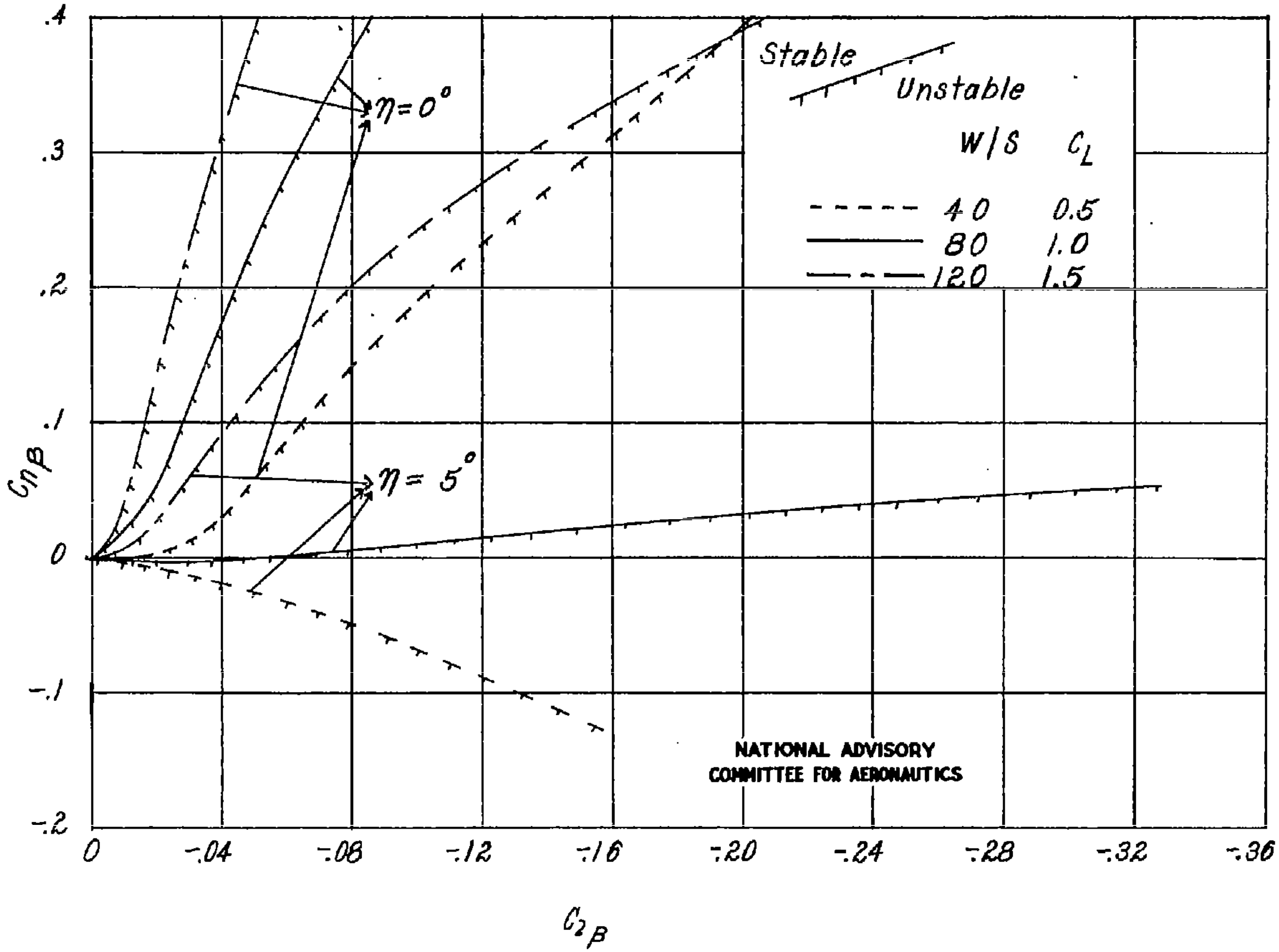


Figure 14.– Effect of wing loading on the oscillatory-stability boundary for landing condition.

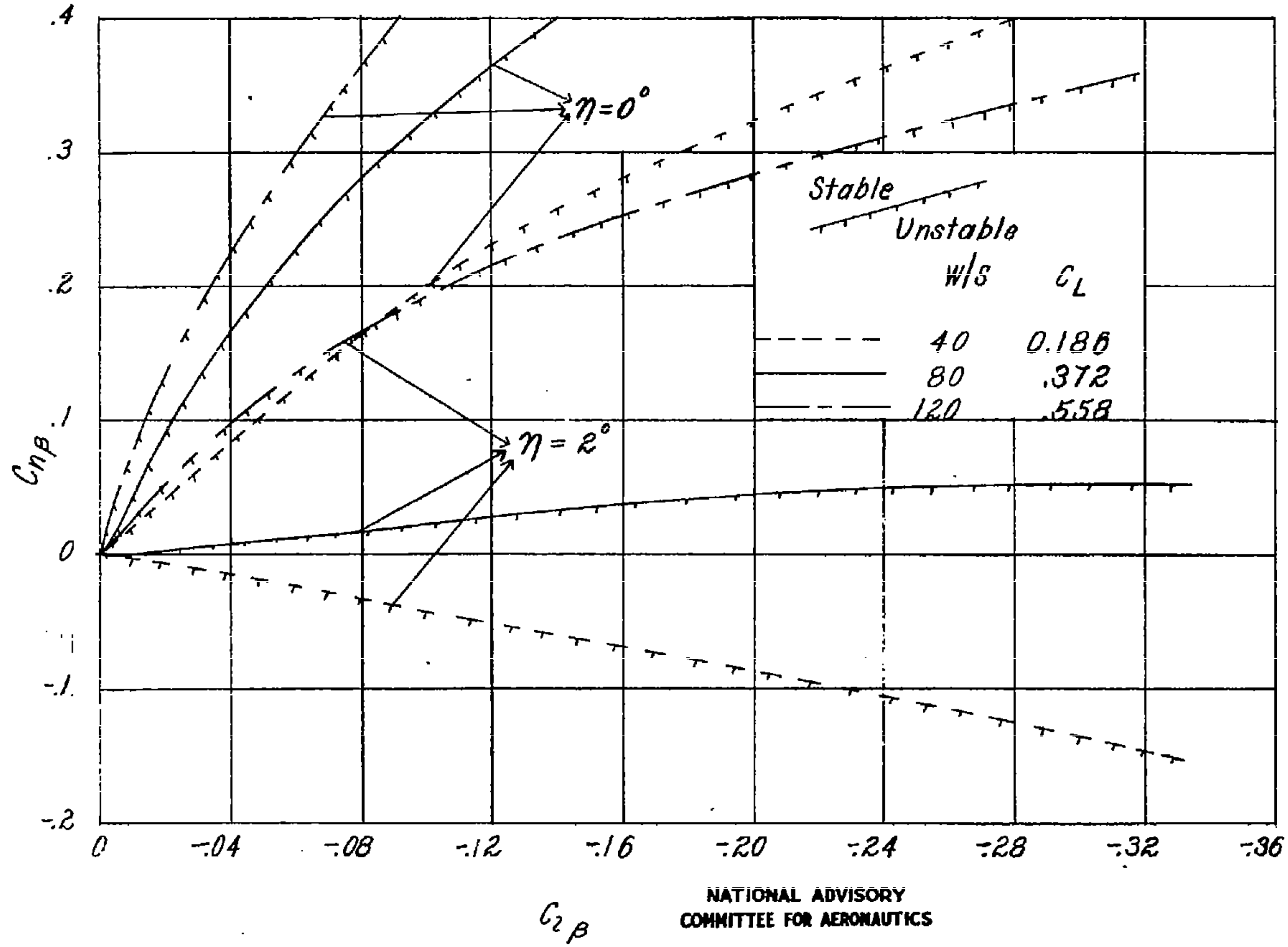


NATIONAL ADVISORY
COMMITTEE FOR AERONAUTICS

Figure 15.—Effect of wing loading on the oscillatory-stability boundary for cruising flight.

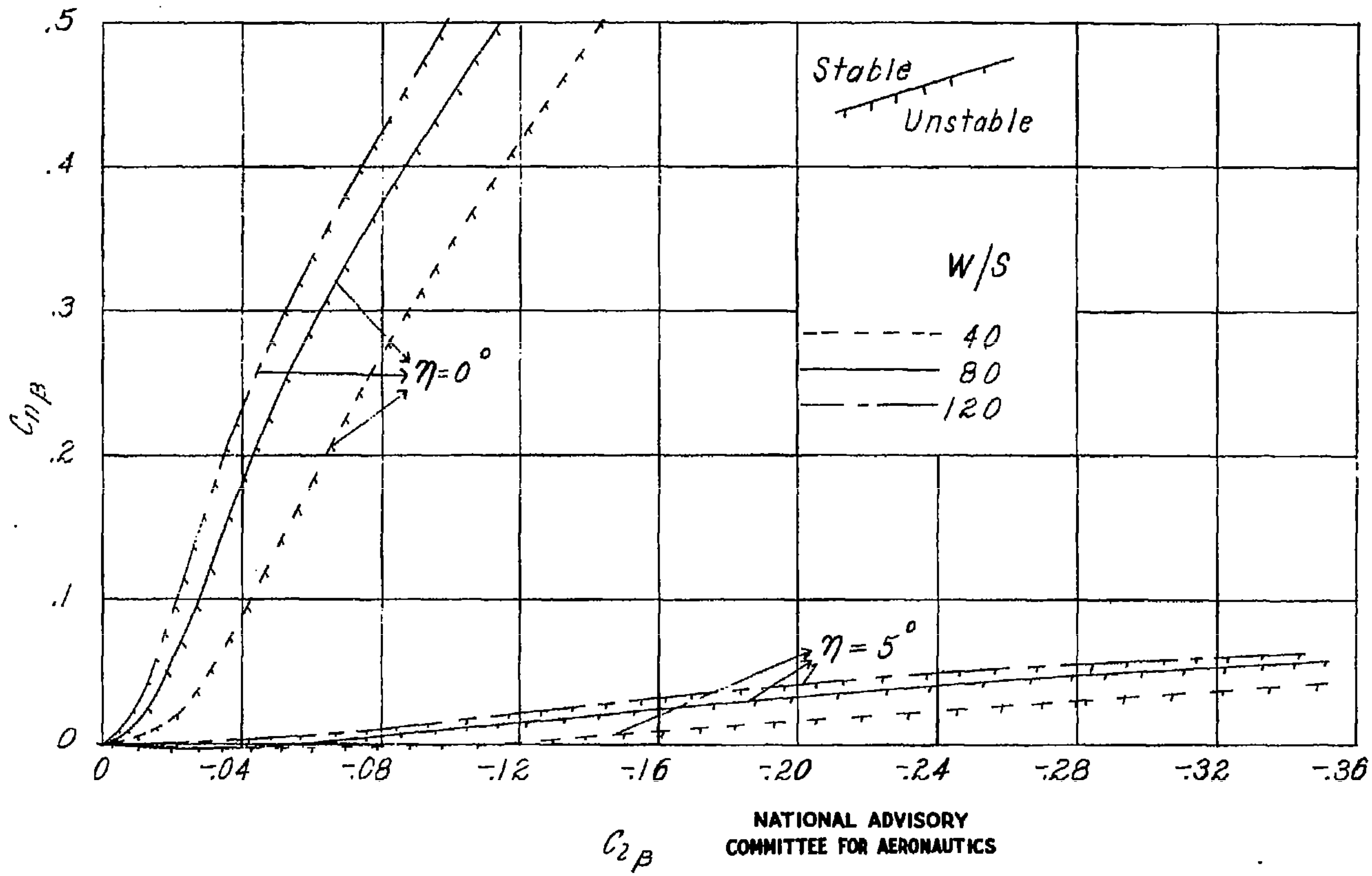


Figure 16.— Effect of wing loading on the oscillatory-stability boundary for landing condition, $C_L = 1.0$.

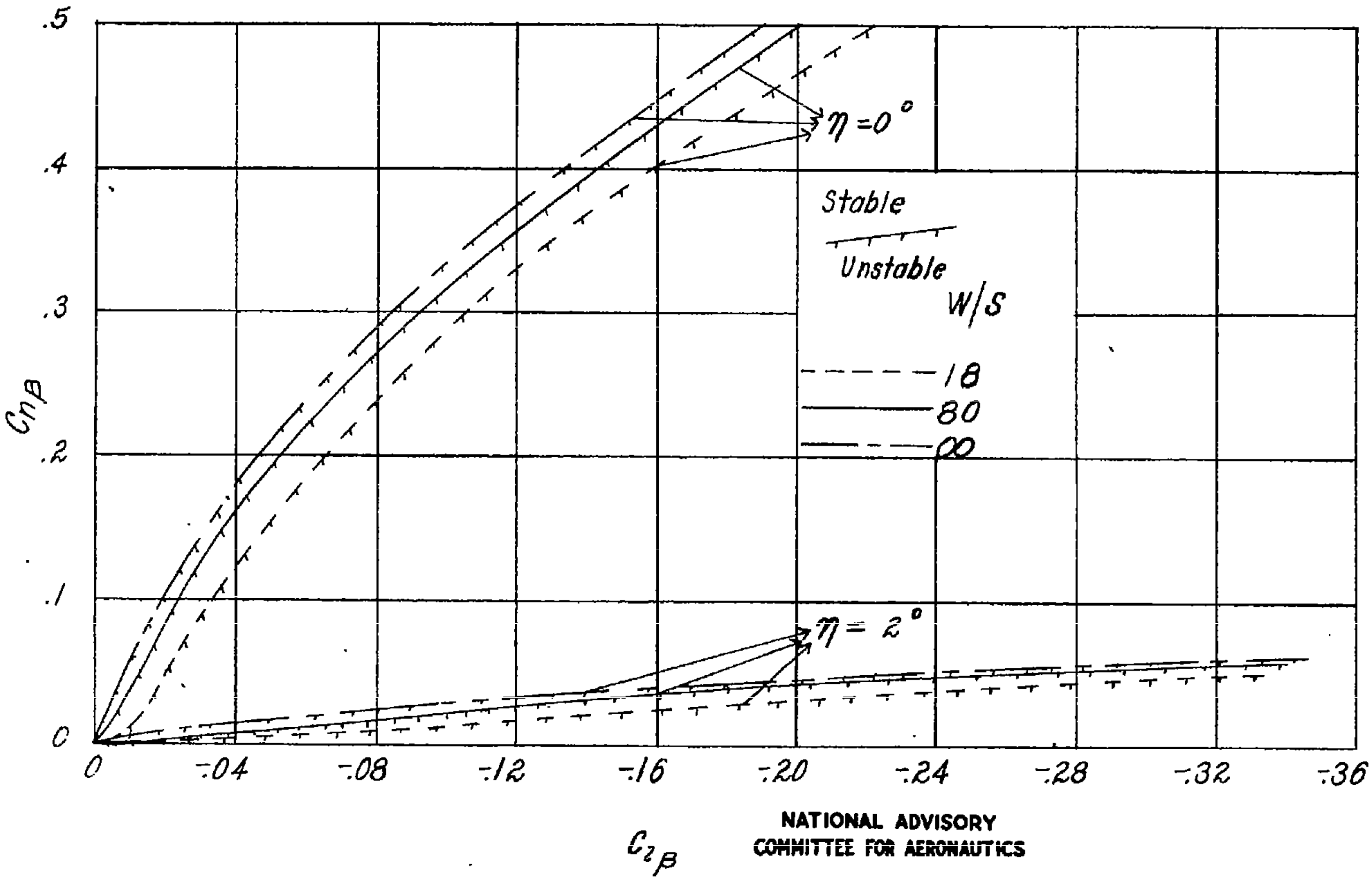


NATIONAL ADVISORY
COMMITTEE FOR AERONAUTICS

Figure 17.—Effect of wing loading on the oscillatory-stability boundary for cruising flight. $C_L = 0.372$.

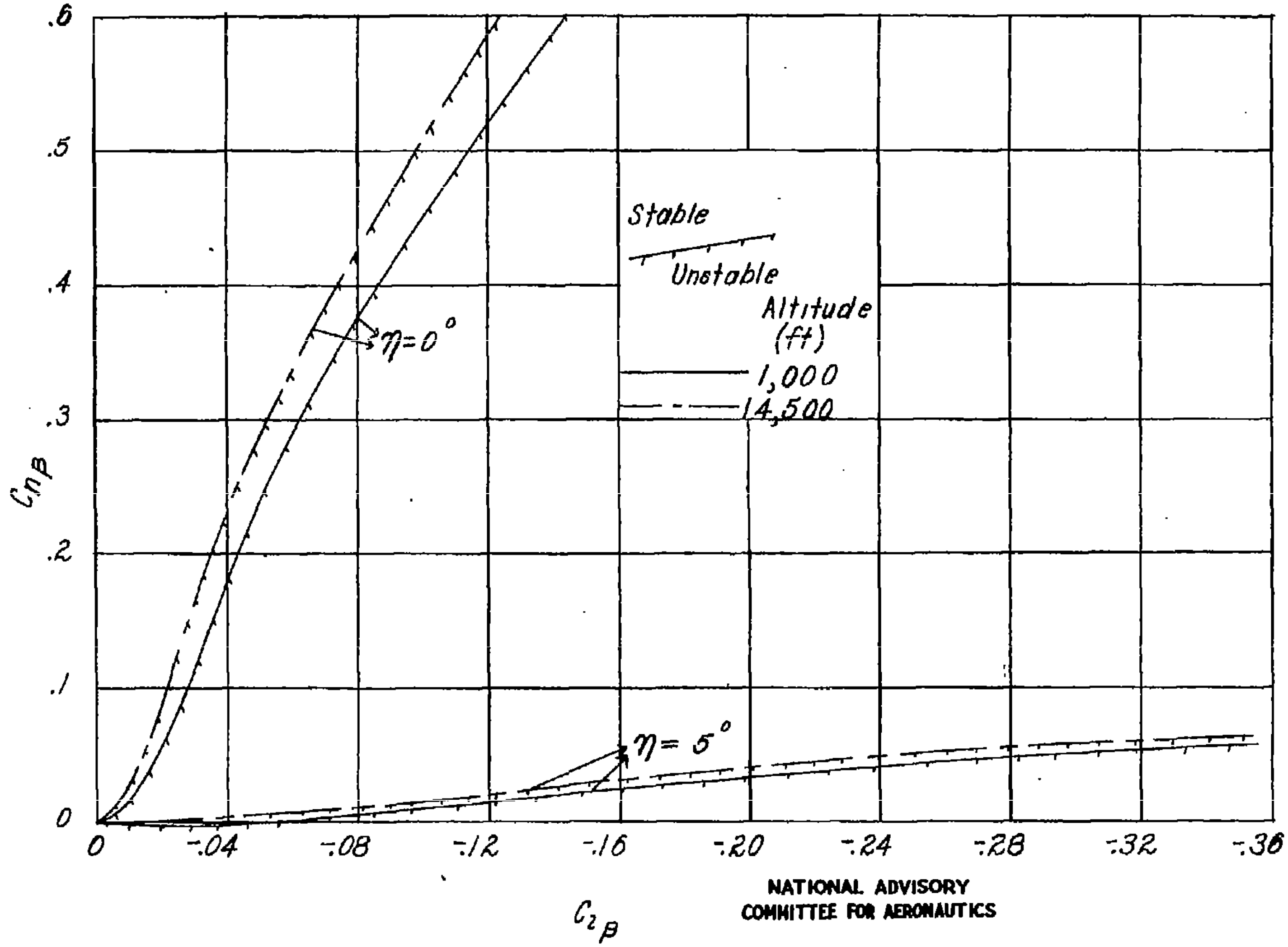


Figure 18.– Effect of altitude on the oscillatory-stability boundary for landing condition. $C_L = 1.0$; $\frac{W}{S} = 80$.

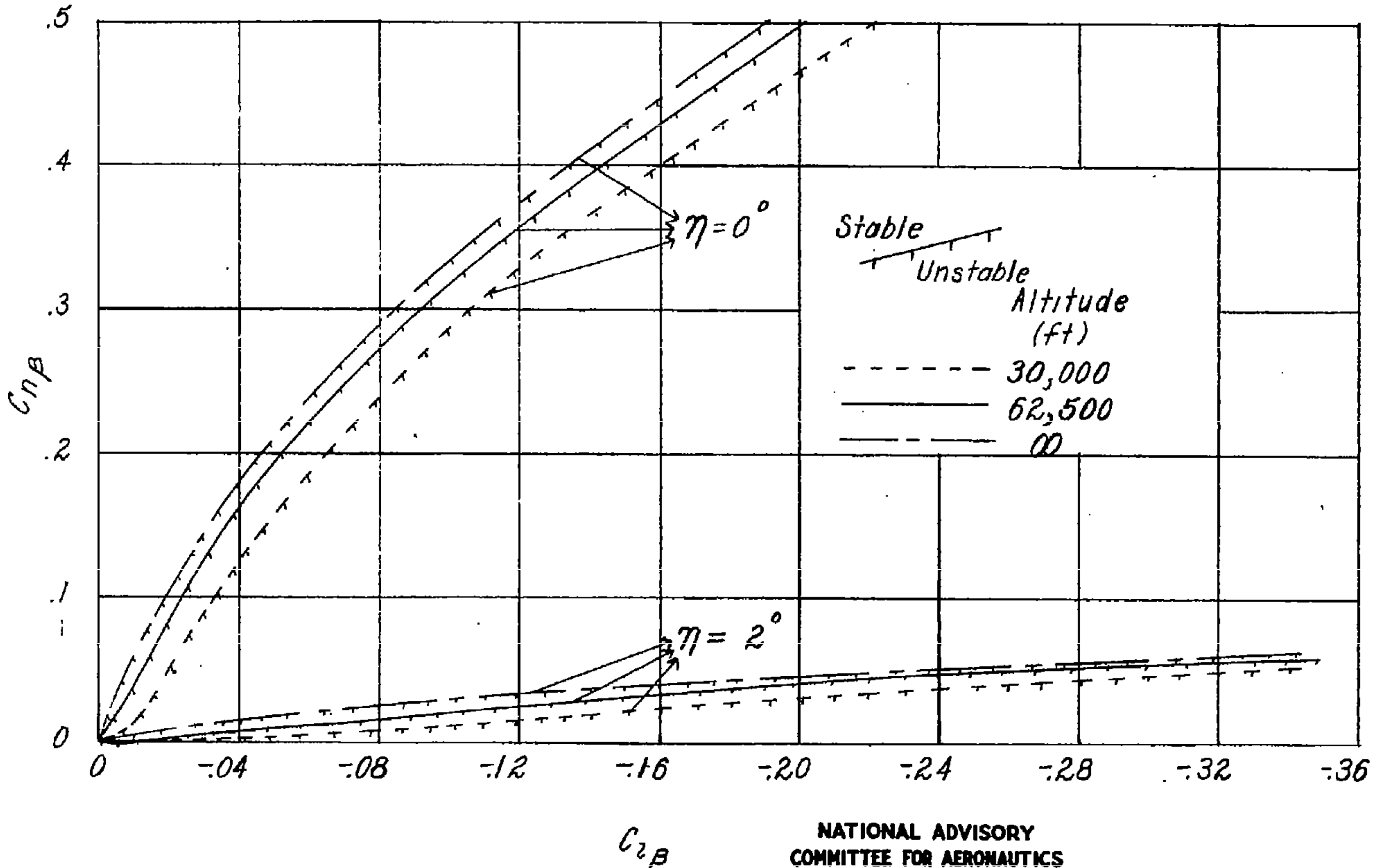


NATIONAL ADVISORY COMMITTEE FOR AERONAUTICS

Figure 19.- Effect of altitude on the oscillatory-stability boundary for cruising flight. $C_L = 0.372$; $\frac{W}{S} = 80$.

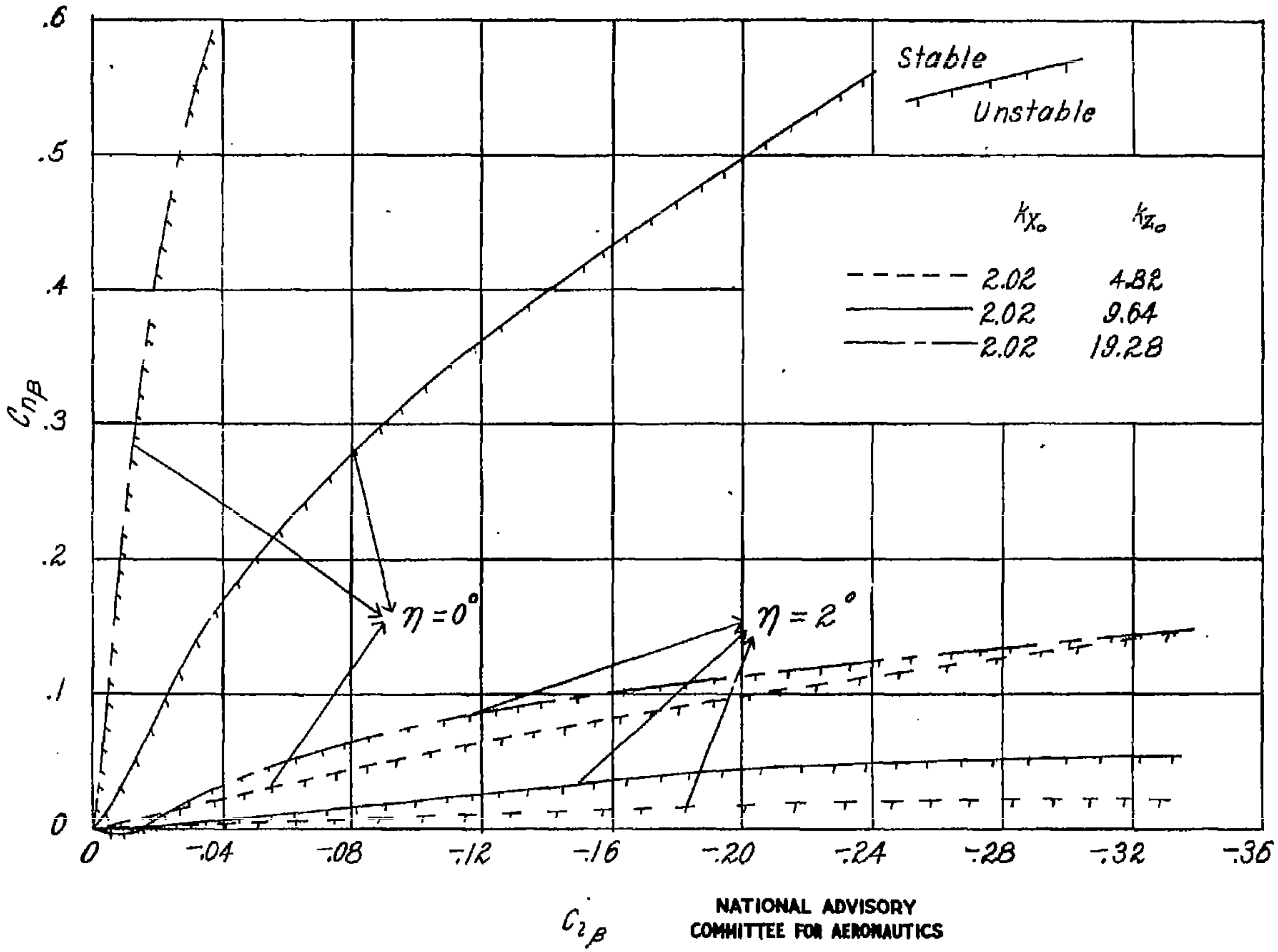


Figure 20.— Effect of radius of gyration in yaw on the oscillatory-stability boundary for cruising flight. $C_L = 0.372$.

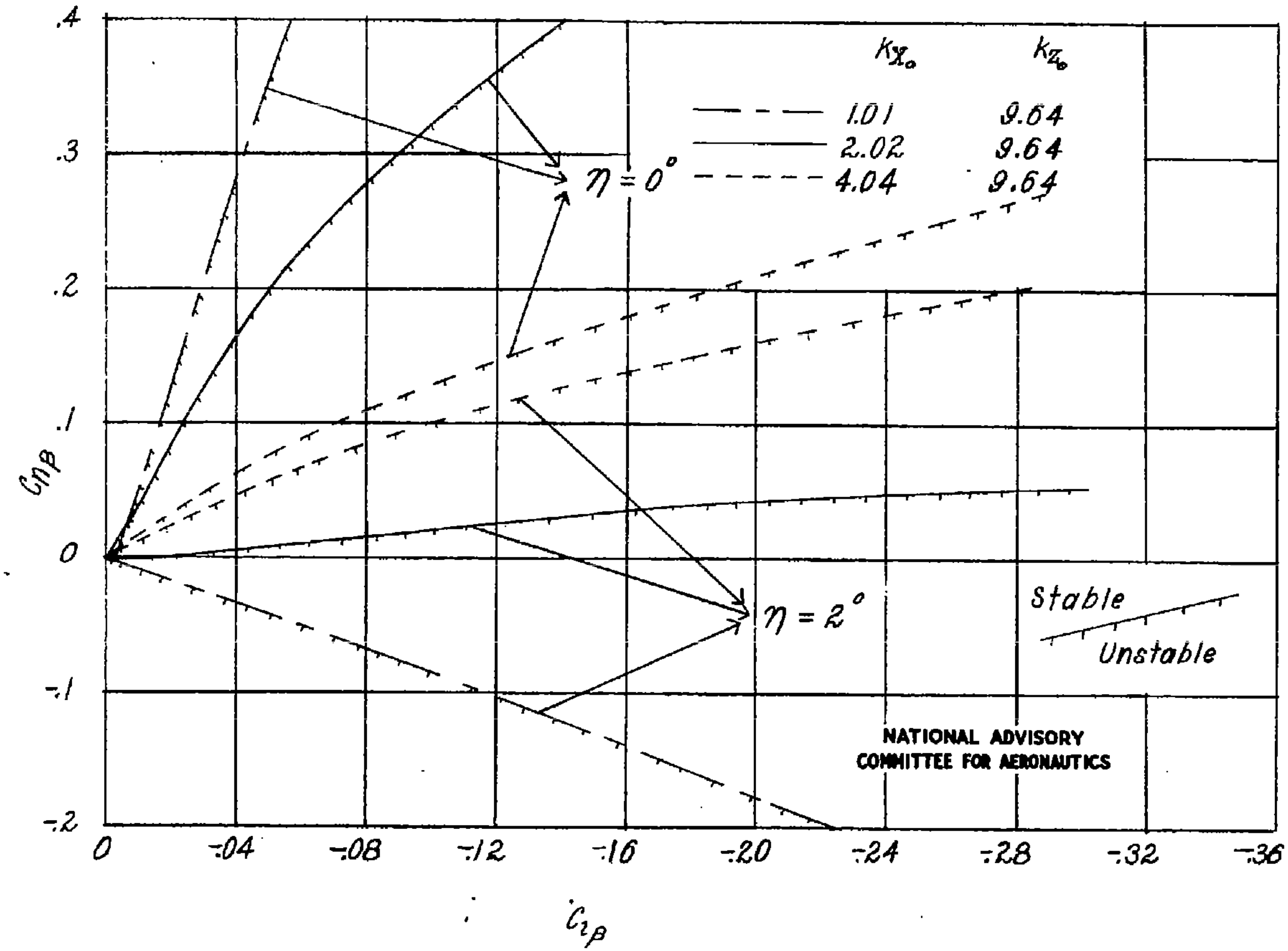


*Figure 21.— Effect of radius of gyration in roll on the oscillatory-stability boundary for cruising flight. $C_L = 0.372$.*

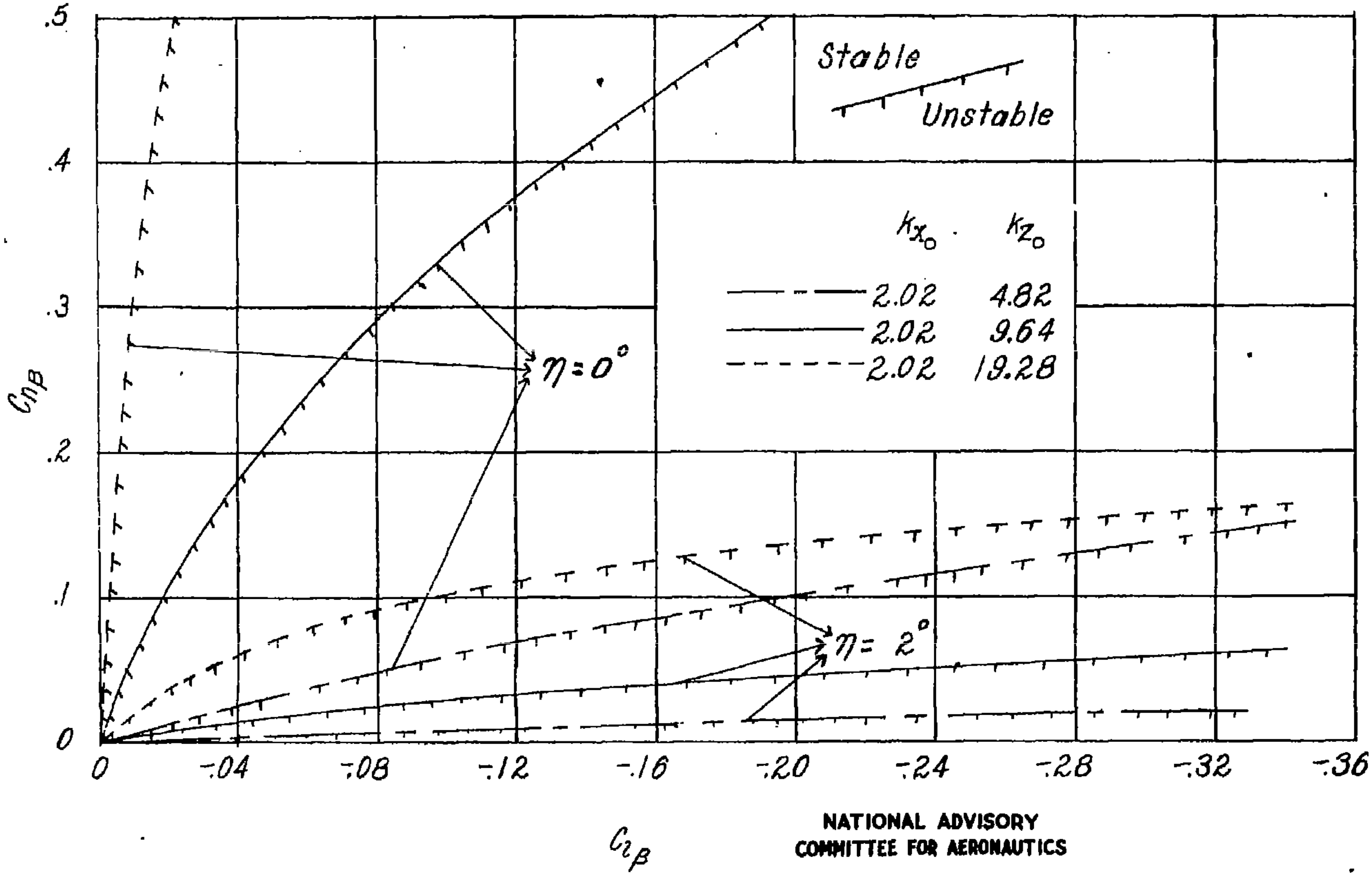


NATIONAL ADVISORY COMMITTEE FOR AERONAUTICS

Figure 22.– Effect of radius of gyration in yaw on the oscillatory-stability boundary for infinite wing loading or altitude at cruising flight. $C_L = 0.372$.

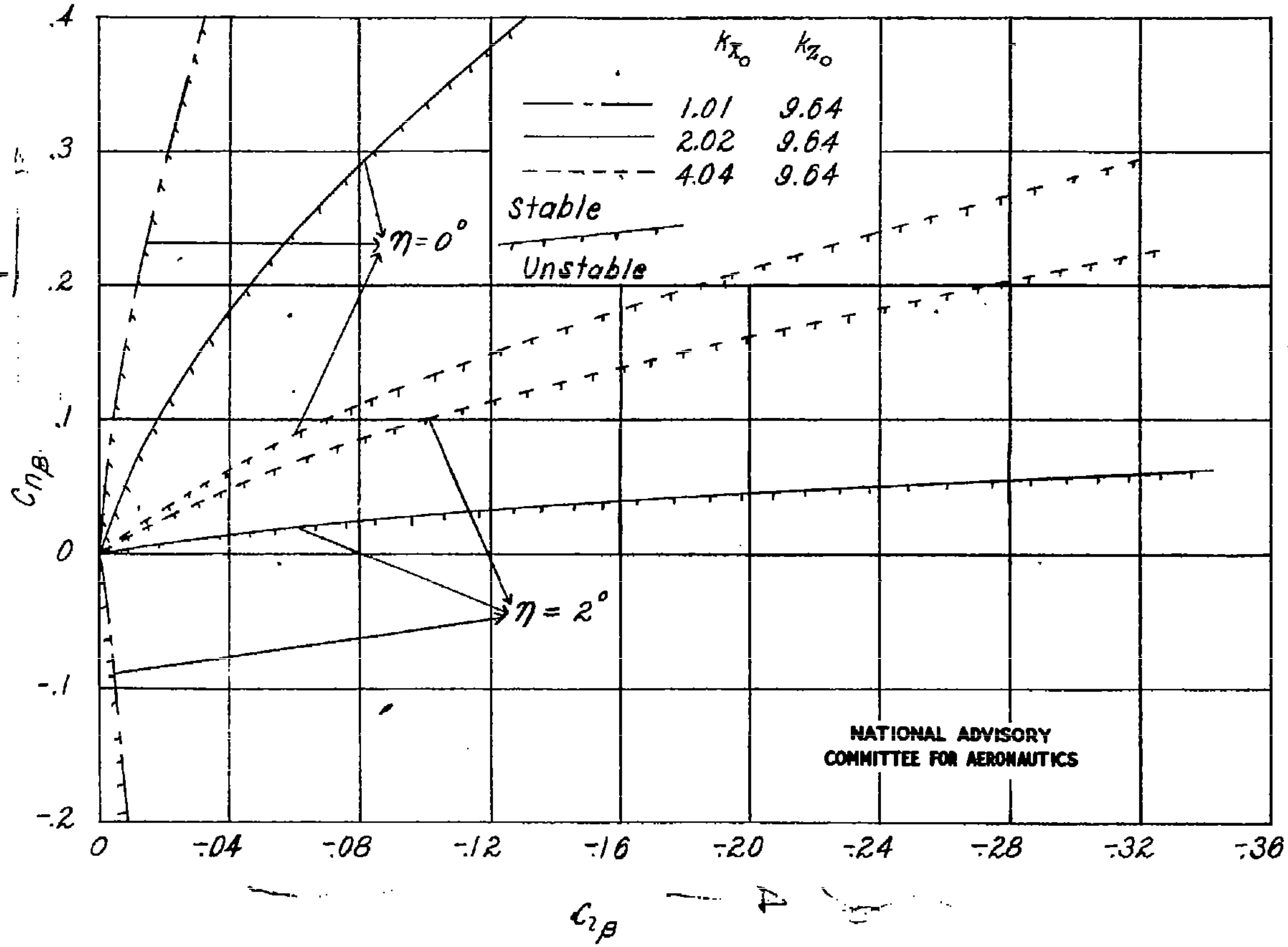


Figure 23.– Effect of radius of gyration in roll on the oscillatory–stability boundary for infinite wing loading or altitude at cruising flight. $C_L = 0.372$.

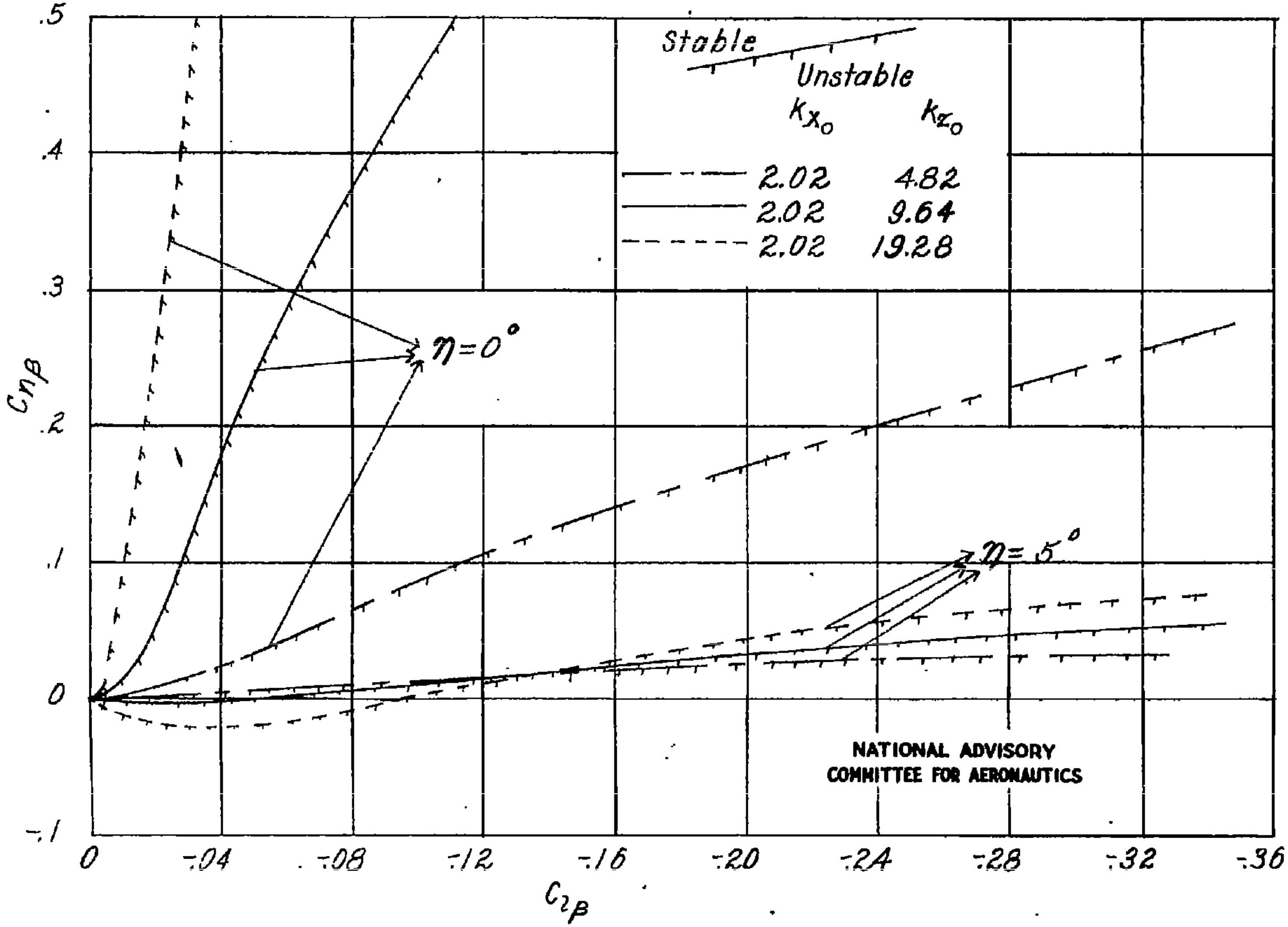


Figure 24.- Effect of radius of gyration in yaw on the oscillatory-stability boundary for landing condition. $C_L = 1.0$.

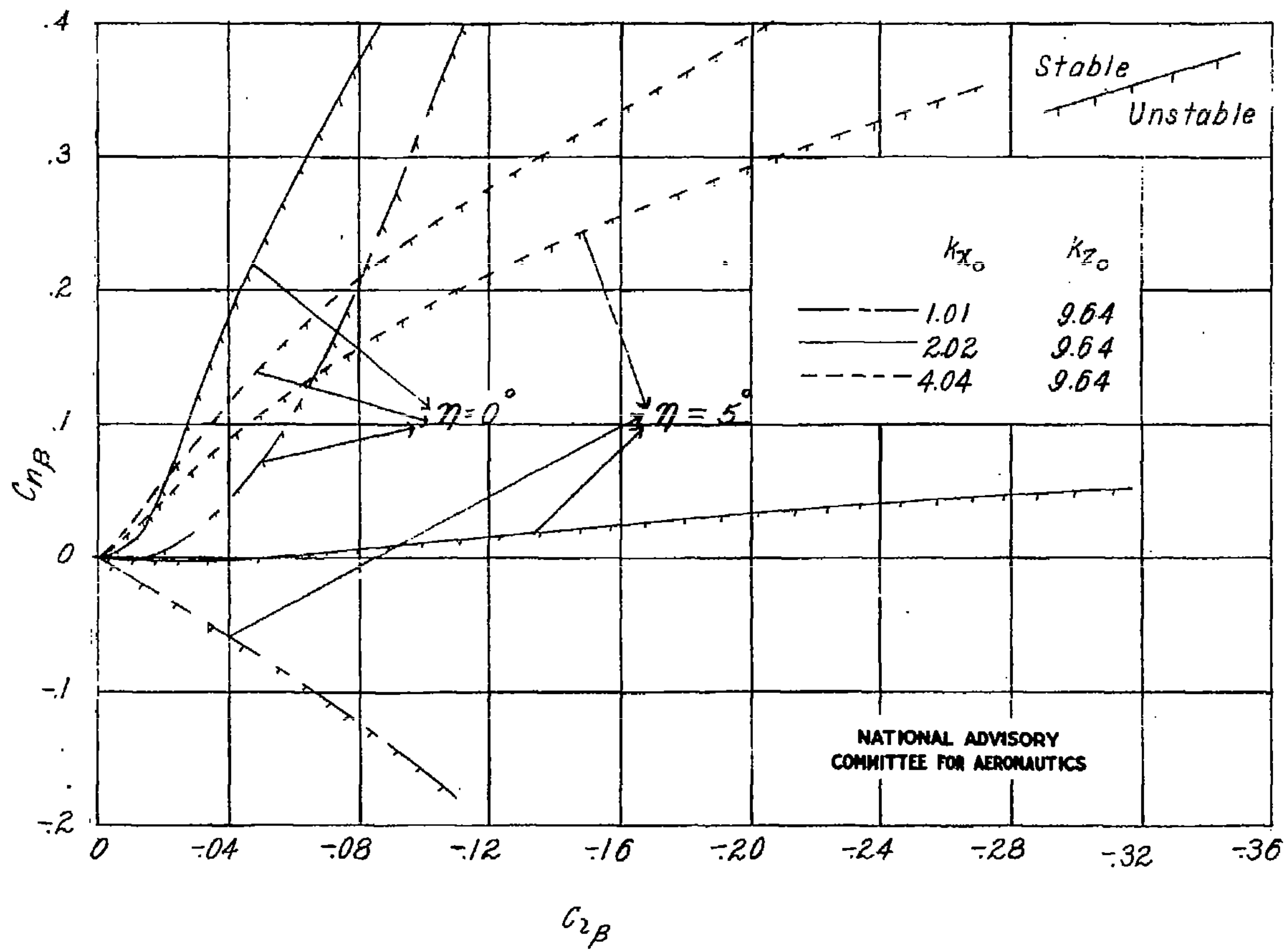


Figure 25.- Effect of radius of gyration in roll on the oscillatory-stability boundary for landing condition. $C_L = 1.0$.

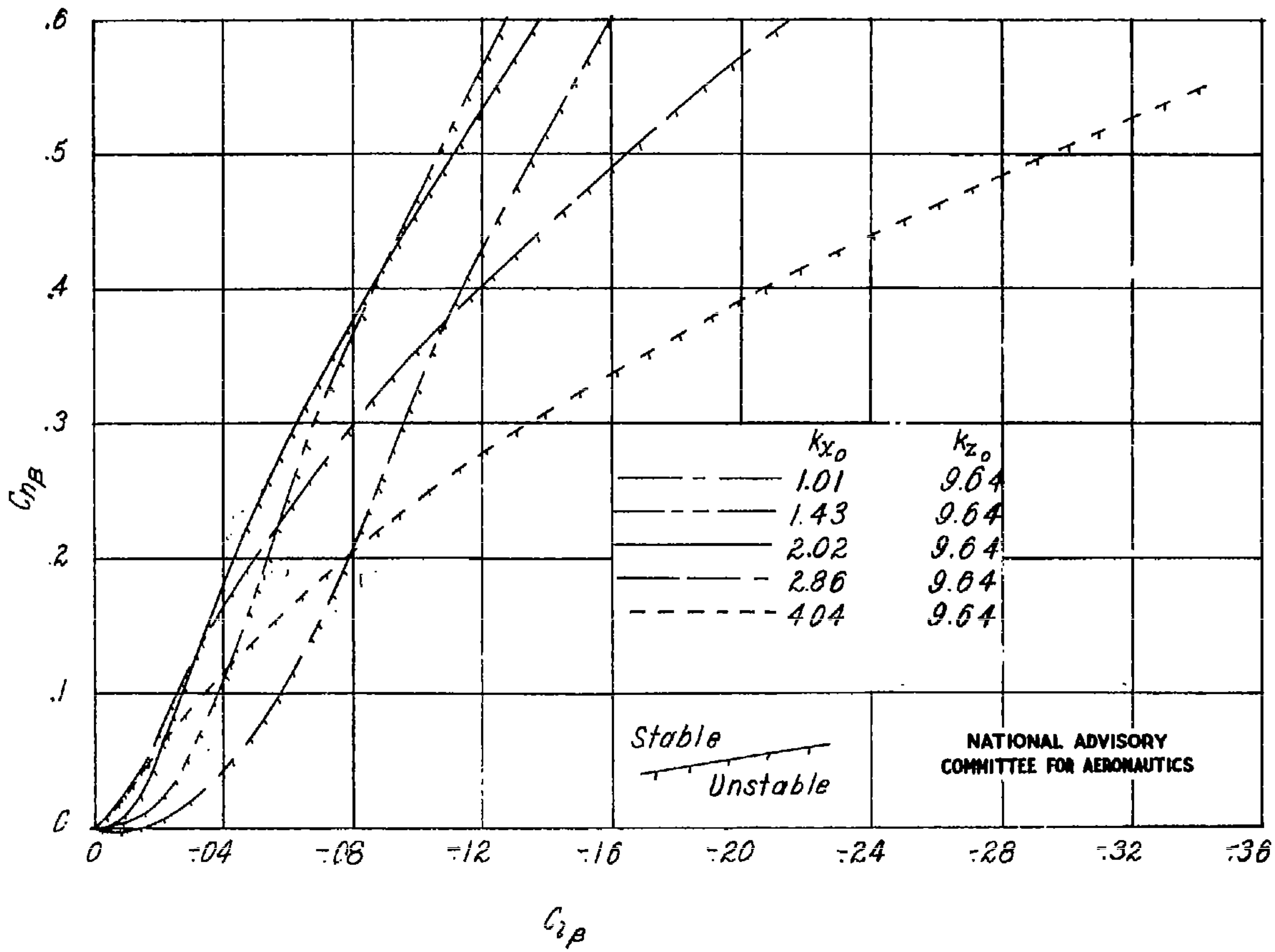


Figure 26.– Effect of radius of gyration in roll on the oscillatory-stability boundary for landing condition. $C_L = 1.0$; $\eta = 0^\circ$.

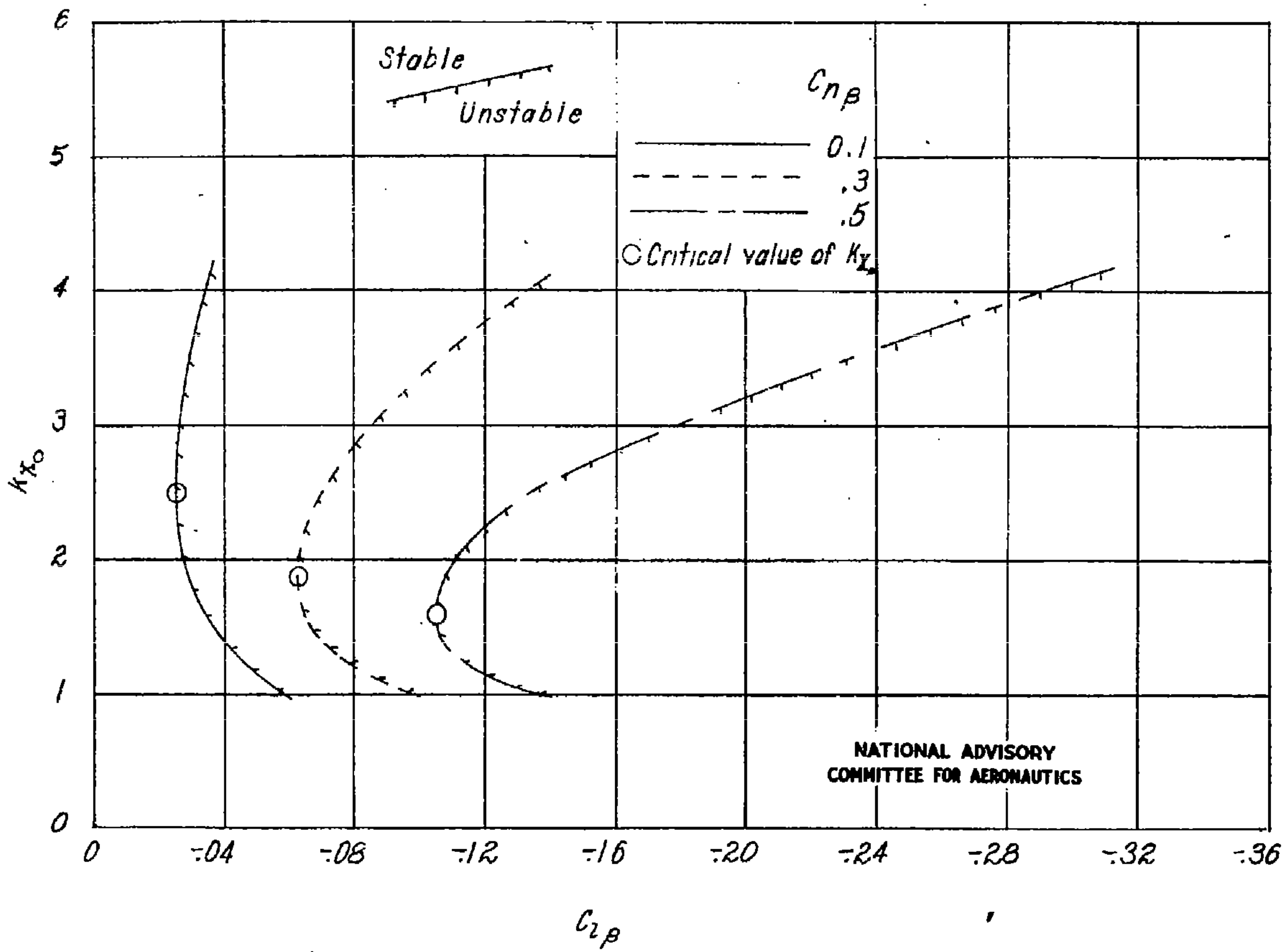


Figure 27.- Effect of radius of gyration in roll on the maximum value of $C_{l_\beta}$ permissible for oscillatory-stability for landing condition. $C_L = 1.0$; $\eta = 0°$.

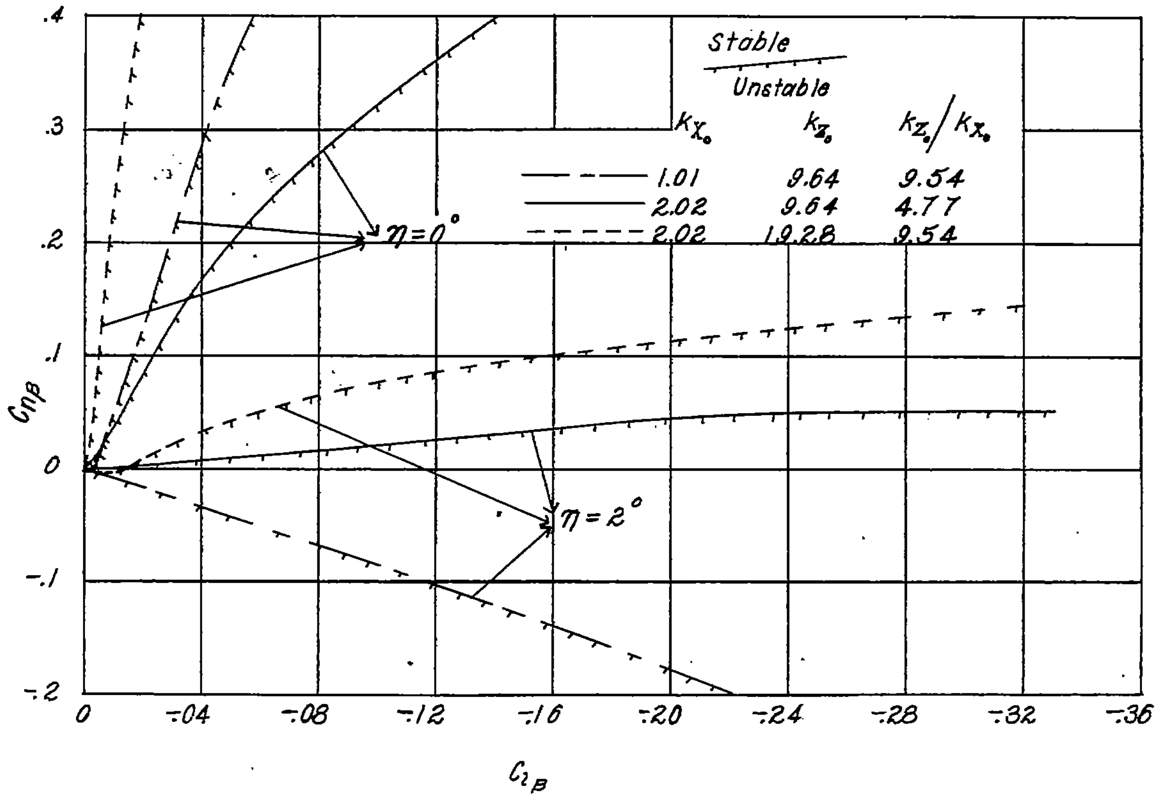


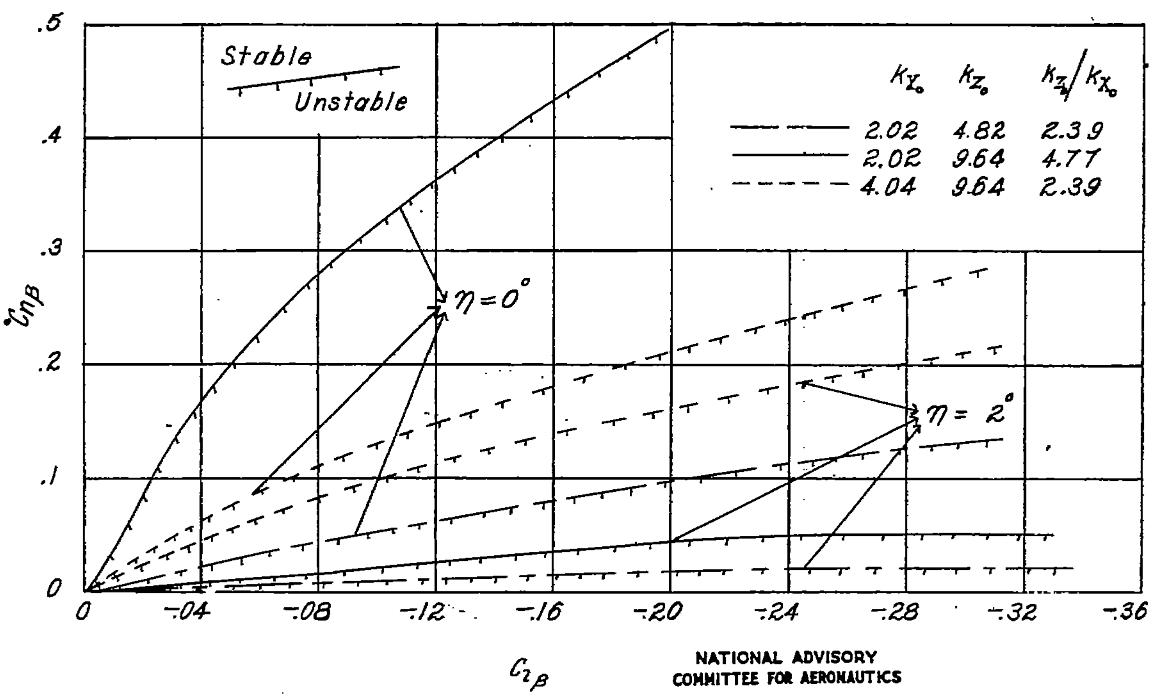


NATIONAL ADVISORY COMMITTEE FOR AERONAUTICS

Figure 28.— Effect of ratio $k_{Z_0}/k_{X_0}$ on the oscillatory-stability boundary for cruising flight. $C_L = 0.372$.

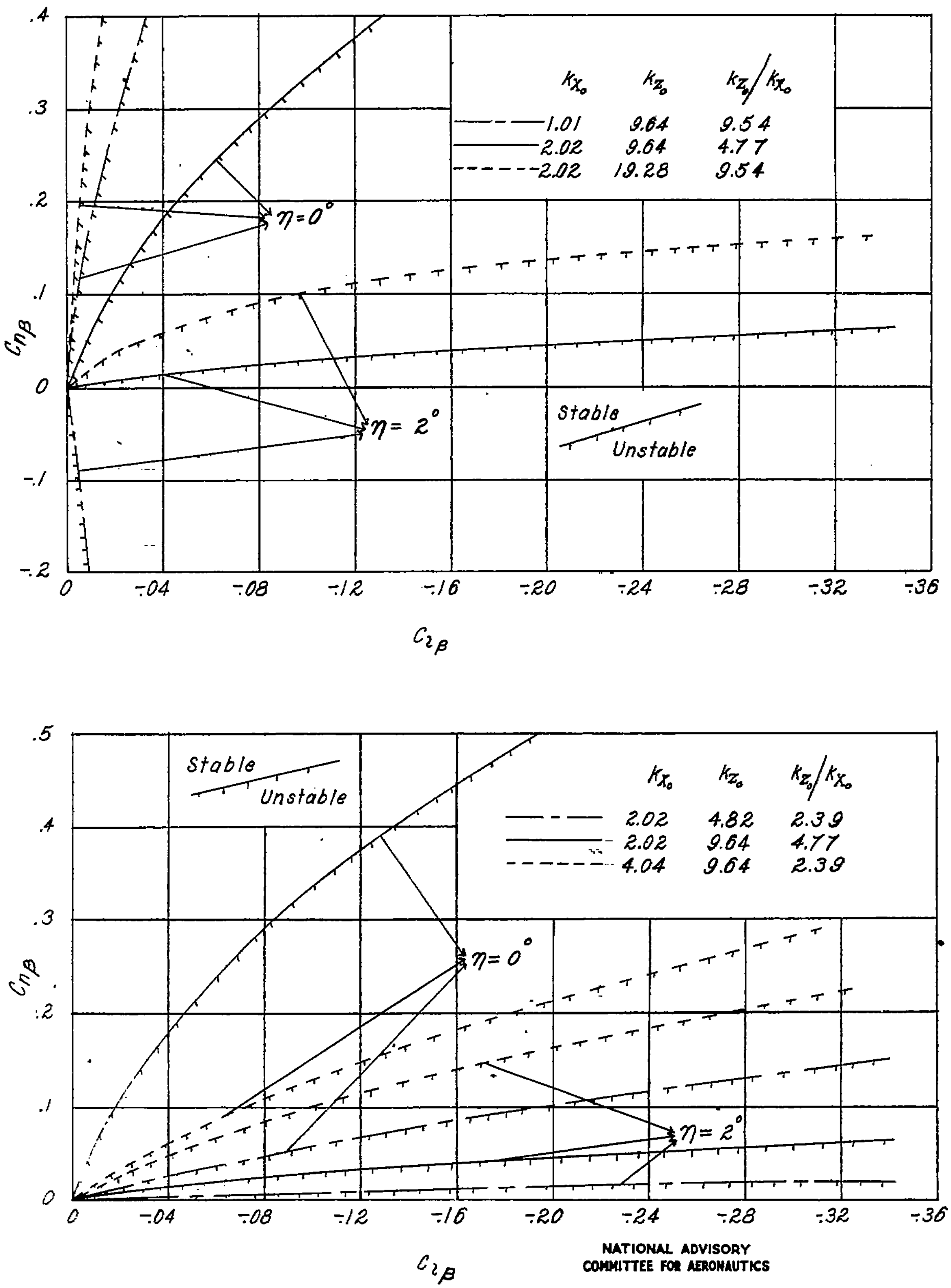


NATIONAL ADVISORY COMMITTEE FOR AERONAUTICS

*Figure 29.— Effect of ratio $k_{Z_0}/k_{X_0}$ on the oscillatory-stability boundary for infinite wing loading or altitude at cruising flight. $C_L = 0.372$.*

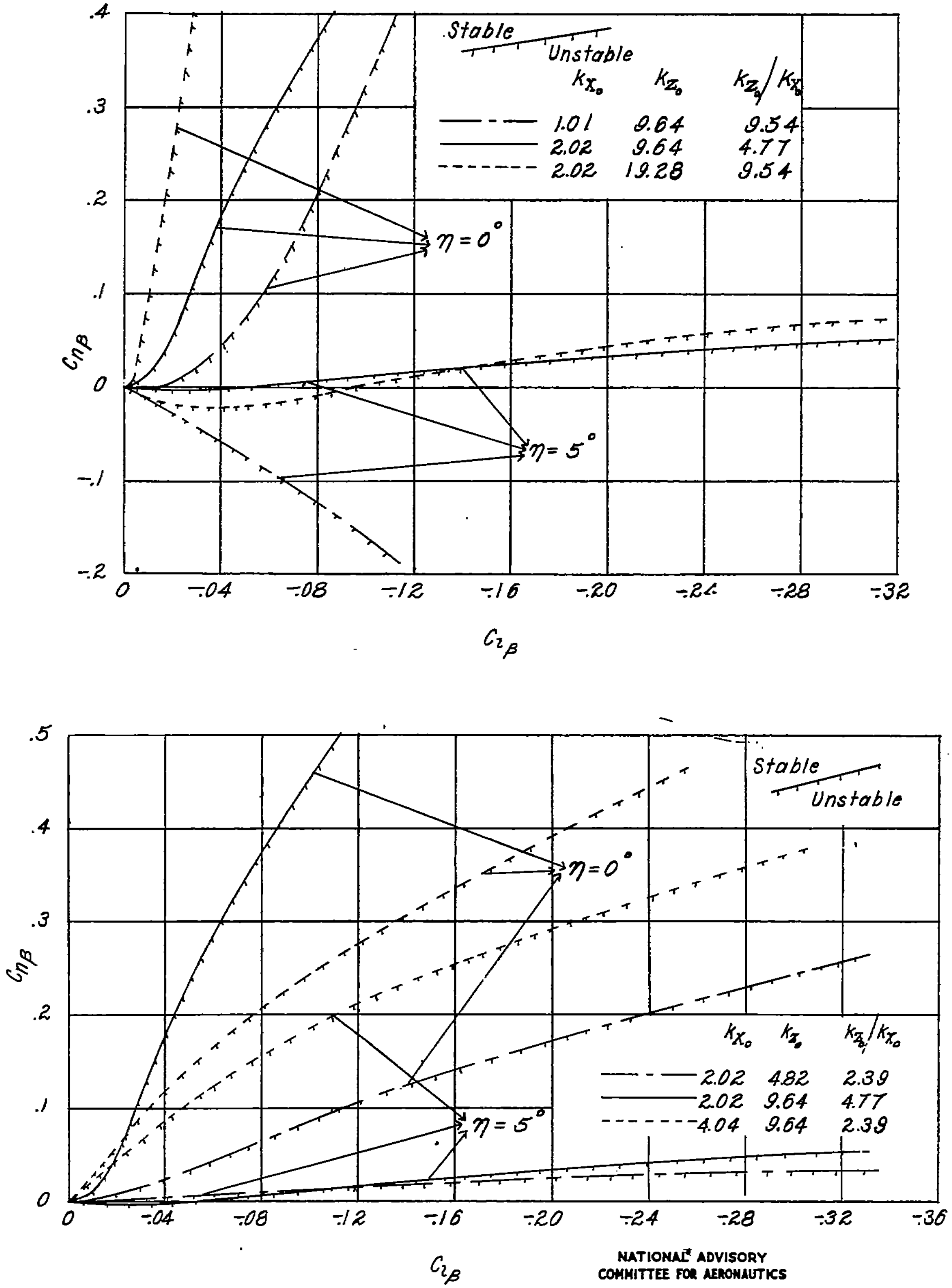


Figure 30.—Effect of ratio $k_{Z_o}/k_{X_o}$ on the oscillatory-stability boundary for landing condition. $C_L = 1.0$.